11-15-2019 10:30 AM

Bioluminescence resonance energy transfer (BRET) - based nanostructured biosensor for detection of glucose

Eugene Hwang
The University of Western Ontario

Supervisor
Zhang, Jin
The University of Western Ontario

Graduate Program in Biomedical Engineering
A thesis submitted in partial fulfillment of the requirements for the degree in Master of Engineering Science

Abstract

Bioluminescence resonance energy transfer (BRET) is a distance dependent, non-radiative energy transfer, which uses a bioluminescent protein to excite an acceptor through resonance energy transfer. In this thesis, BRET technology is incorporated into a sensor comprised of a recombinant protein and quantum dots. The recombinant protein, which includes the bioluminescent protein, *Renilla luciferase* (Rluc), is used as the donor molecule and cadmium tellurium quantum dots as the acceptor molecules. Separating the donor-acceptor pair is a recombinant protein, glucose binding protein, which changes conformation upon binding glucose and brings the pair closer together, thus allowing BRET to occur. Optimization of the BRET sensor was investigated by evaluating different ratios of the donor and acceptor, changes in the bioconjugation process, and different glucose concentrations. The intensity of bioluminescence is a function of the ratio between the quantum dots to protein, which ranges from 1:6 to 0.0156:1, EDC ratio to quantum dots, conjugation time, and concentration of glucose ranging from 2 μM to 0.1 M. In addition, the performance of the sensor on a solid substrate was evaluated. This sensor promises to offer an alternative to traditional blood glucose sensing.

Keywords

Bioluminescence resonance energy transfer, BRET, Renilla luciferase, Quantum dots, Glucose sensing

Summary for Lay Audience

Type 1 diabetes is a disease characterized by loss of blood glucose control due to autoimmune destruction of pancreatic beta islet cells. Modern treatment requires the use of a blood glucose meter, often requiring the pricking of the finger. Constant pricking is a detriment to the quality of life to these patients and may lead to decreases in patient adherence. The goal of this project is to develop a non-invasive alternative to measuring blood glucose by utilizing tears. A newly designed sensor using a technology known as bioluminescence resonance energy transfer (BRET) has been developed with the hopes that it may replace traditional glucose sensing methods. BRET occurs when a light emitting protein transfers light energy to another light emitting protein. The second protein will then emit its own light, which can then be measured. The newly designed sensor uses quantum dots in the place of a second protein due to unique properties that make them suitable for glucose sensing. The sensor components are separated by a glucose binding protein, which changes conformation upon binding glucose. Therefore, the amount of light emitted by the quantum dot will correspond to whether glucose has bound the sensor. Testing of the sensor revealed that a 0.3125:1 ratio of the protein to quantum dots to be ideal. In addition, the sensor could detect variations of glucose levels ranging between 2 μM to 0.1 M, which is sufficient to detect levels of glucose in both tear samples and blood samples. The sensor was also tested while deposited on a solid substrate. The results indicate the sensor may be promising as an alternative to traditional blood glucose sensing.

Co-Authorship Statement

All chapters were written by Eugene Hwang with contribution by JiSu Song in chapter 2 in regards to details on bioluminescence proteins and Songlin Yang with contribution in chapter 6 in regards to synthesis of the ZnO nanorod array on PDMS. Reviewing and editing was done throughout the thesis by Dr. Jin Zhang.

Acknowledgments

I would like to extend my gratitude to all of those who were instrumental in seeing the project to its conclusion. Their help was invaluable and the project would not have been possible without their contributions.

Firstly, I would like to acknowledge my supervisor, Dr. Jin Zhang, who has been essential for her mentorship and guidance throughout my master's program. She has always offered valuable insight to my project even when times were uncertain and I was struggling. Without her encouragement and advice, I would not have been able to finish the project.

Secondly, my appreciation goes out to the members of my advisory committee, Dr. Jun Yang and Dr. Sohrab Rohani. Their feedback and advice were greatly appreciated.

Finally, special thanks to my colleagues at the Multifunctional Nanocomposite Lab who include Songlin Yang, JiSu Song, Yingqi Zhang, Chao Lu, Aditya Balaji, Longyi Chen, Denghuang Zhan, Andrew Tse, and Deepthi Muraleedharan. I wish to thank them for their unwavering support and contributions made to the benefit of my project.

I would like to acknowledge the support from Natural Science and Engineering Research Council of Canada (NSERC) through a Discovery Grant and Western Engineering Graduate Scholarship.

Table of Contents

List of Tables

List of Figures

List of Abbreviations

BCA	-	Bicinchoninic acid assay
BRET	-	Bioluminescence resonance energy transfer
CdSe	-	Cadmium selenide
CdTe	-	Cadmium telluride
CRET	-	Chemiluminescent resonance energy transfer
EDC	-	1-ethyl-3-(3-dimethylami-nopropyl) carbodiimide
Fluc	-	Firefly luciferase
FRET	-	Fluorescence resonance energy transfer
GBP	-	Glucose binding protein
Gluc	-	*Gaussia* luciferase
IPTG	-	isopropyl β-D-1 thiogalactopyrandoside
LB broth	-	Luria-Betrani broth
Lux	-	Bacterial luciferase
Nluc	-	Nano luciferase
PDMS	-	Polydimethylsiloxane
PPI	-	Protein-protein interaction
QD	-	Quantum dot
Rluc	-	*Renilla* luciferase
SDS-PAGE	-	Sodium dodecyl sulfate polyacrylamide gel electrophoresis
TGA	-	Thioglycolic acid

UV	-	Ultraviolet
Vluc	-	*Vargula* luciferase
λ_{cm}	-	Emission wavelength (nm)

List of Appendices

Chapter 1

1 Introduction

1.1 Glucose sensors in diabetes

Type 1 diabetes is a metabolic disorder characterized by loss of blood glucose control due to the autoimmune destruction of insulin-producing beta islet cells. This loss of blood glucose control can lead to a variety of complications due to hyperglycemia. Many diabetic patients are at increased risk of cardiovascular and neurovascular disease. Careful and accurate monitoring of blood glucose is essential for patients with type 1 diabetes in order to reduce the risk of hypoglycemia and other related complications [1]. Traditional blood glucose monitoring techniques utilize a blood glucose meter. These meters require the pricking of the patient's finger to obtain a small blood sample [2]. This method is a detriment to the quality of life to these patients, as constant pricking throughout the day is often painful and inconvenient. Constant pricking may decrease patient adherence to treatment, therefore current efforts have focused on the development of a non-invasive means of glucose monitoring [3].

Recent works have investigated the measurement of changes in blood glucose as they related to changes in other related chemical and physical properties of the body. For example, changes in other body fluids such as urine [4,5], sweat [6–8], and tears [9,10] have provided new avenues to assess changes in blood glucose in a non-invasive manner. Due to significantly lower values of glucose in related body fluids, methods with increased sensitivity need to be developed in order to accurately measure glucose levels.

The most popular traditional glucose biosensors are based on glucose interactions with enzymes such as glucose oxidase (GOx) [11]. Also known as enzymatic amperometric sensors, these sensors use immobilized GOx to oxidize glucose which forms hydrogen peroxide [12]. The hydrogen peroxide is oxidized at a catalytic, platinum anode where the electrode can recognize the number of electron transfers. The electron flow is proportional to the number of glucose molecules present in the medium [13].

Glucose biosensors are designed to be used for point-of-care testing and are easily operated by outpatients [14]. However, the American Diabetes Association recommends that the accuracy of such biosensors should be less than 5% of the measured value, which many devices fail to achieve. Therefore, along with the benefit of a non-invasive alternative, a more accurate biosensor version could prove to be of significant value.

Traditional biosensors are limited in their signal capture efficiency of a biological recognition event. Therefore, the use of nanomaterials in biosensors has become more popular. Due to their lower detection limits, ability to immobilize an increased quantity of bioreceptor units at a reduced volume, and ability to act as a transduction element, nanomaterials are very promising for use in biosensors [15].

Methods with increased sensitivity have been explored, particularly using fluorescence resonance energy transfer (FRET). However, such methods require the use of an external energy source which is difficult to implement within a biological environment [16]. Therefore, bioluminescence resonance energy transfer (BRET) has been explored as an alternative that does not require an external energy source and are therefore not limited in their applicability in biological settings [17–19].

1.2 Resonance energy transfer

Bioluminescence resonance energy transfer-based sensors offer a high degree of sensitivity and reliability in a procedure that is both easy to perform and relatively inexpensive. BRET sensors utilize bioluminescence generated from a luciferase enzyme found in the sea pansy in order to donate energy to a fluorescence molecule that will emit a measurable quantity of fluorescence [17–19]. This system can be used to monitor an easily detectable light signal in real time with a high degree of sensitivity. BRET sensors are a less invasive and easier to perform modification of fluorescence resonance energy transfer which requires an external light source to initiate the fluorescence transfer [16]. No longer requiring an external light source has made BRET attractive for use in biological systems. Limitations of a fluorescence-based sensor include

tissue autofluorescence and photobleaching. Background emission from tissue, otherwise known as autofluorescence, was found to be a limiting factor in the sensitivity of reporters [20–22]. Research has reported significantly higher autofluorescence levels in fluorescent reporters when compared to bioluminescent reporters [21,23]. Chemiluminescent resonance energy transfer (CRET) is a related technique that relies on the oxidization of a chemiluminescent compound which will excite an acceptor fluorophore [24,25]. There are a limited number of studies done using CRET, therefore its efficacy and biocompatibility have not been adequately proven [26,27]. Thus, the use of bioluminescent reporters has become increasingly attractive in biological applications.

BRET is a natural phenomenon involving the non-radiative energy transfer between a bioluminescent donor molecule and a fluorescent acceptor molecule. When the bioluminescent donor, typically an oxidative luciferase enzyme, emits bioluminescent energy, this excites the fluorescent acceptor and increases its emission [22,28]. This is referred to as resonance energy transfer and only occurs when the two proteins are within 10nm (Figure 1.1) [23]. The changes in ratio of the acceptor to donor emissions are monitored which are useful in studying protein-protein interactions (PPI) since the mechanism depends on distance [16,22].

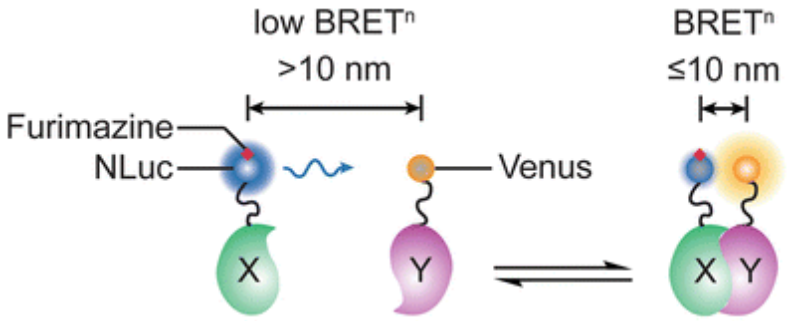

Figure 1.1: Schematic of a NanoLuc (NLuc) based BRET (BRETⁿ) design. Nluc is the donor fluorophore and Venus is the acceptor fluorophore. Nluc and Venus are fused to their respective proteins of interest (X and Y). BRET signal is detected when the proteins are in close proximity. Reprinted by permission from Springer Nature [23]. Copyright 2016.

FRET and, by extension, BRET, is a distance dependent mechanism. The efficiency of the energy transfer (*E*) is defined as the quantum yield of the energy transfer transition [29]. The efficiency depends on the distance between the donor and acceptor, usually up to 10 nm. In addition, the emission spectrum of the donor should overlap with the acceptor's absorption spectrum. The donor emission dipole moment and the acceptor absorption dipole moment should be relatively oriented [30,31]. The efficiency is calculated using equation (1.1):

$$E = \frac{R_0^6}{R_0^6 + r^6} \tag{1.1}$$

Where *r* is the distance between the donor and acceptor and R_0 is the Förster distance of the donor acceptor pair which is the distance where E = 50%.

The Förster distance is given by equation (1.2):

$$R_0 = 0.21[\kappa^2 Q_D n^{-4} J(\lambda)]^{\frac{1}{6}} \tag{1.2}$$

Where J(λ) is the spectral overlap between donor emission and acceptor absorption, Q_D is the quantum yield of the donor, n is the refractive index of the medium, and κ^2 is an orientation factor related to the relative orientation of the donor emission and acceptor absorption dipole moments.

Many limitations must be taken into consideration when constructing a BRET sensor system. Conventional BRET systems utilize bioluminescence proteins as donor molecules and organic dyes as acceptor molecules. However, suitable BRET pairs utilizing organic dyes are often limited due to narrow emission wavelengths of the dyes [22]. In order to increase the flexibility of the acceptor molecule, quantum dots have been incorporated in the place of organic dyes. Quantum dots offer a wealth of advantages, in particular, a tunable emission wavelength. Therefore, the challenges of constructing a BRET sensor system can be overcome using inorganic nanomaterial as acceptor molecules.

1.3 Bioluminescent proteins

There exists a variety of bioluminescence donors, many of which are derived from naturally occurring enzymes in animals such as the firefly or the sea pansy. Among the different donors, each has clear advantages and disadvantages in certain applications. Therefore, certain donors are considered for certain tasks according to their properties.

Commonly used bioluminescence donors include the luciferases, a class of oxidative enzymes, which catalyze the oxidative decarboxylation of luciferin. Luciferins are light-emitting compounds that generate bioluminescence upon undergoing oxidation, which results in the emitting of light upon decaying from an excited state to its ground state. Upon oxidation of the luciferin in the presence of oxygen, carbon dioxide, oxyluciferin (III) and light are released [32].

1.4 Quantum dots

Quantum dots (QD) are light-emitting semiconductor nanocrystals with optical and electrical properties. Applications for QDs range from bioanalytical assays, live cell imaging, fixed cell and tissue labeling, biosensors and *in vivo* animal imaging [33]. The fluorescence properties of QDs are determined by the core materials and the shell layer, which removes surface defects and prevents nonradiative decay [34]. The optical property of QD is a result of the quantum confinement effect of semiconductor materials. The quantum confinement effect refers to the size and composition dependent properties of the semiconductor gap energy. Nanocrystals smaller than the Bohr excitation radius have quantized energy levels which depend directly on the size of the nanoparticle. This allows the development of fluorescence emitters with precisely tuned emission wavelengths. For example, cadmium selenide (CdSe) has a bandgap of 1.7 eV (corresponding to 730nm light emissions). Through the altering of the nanocrystal diameter from 2 to 7nm, the QD can be tuned to emit between 450 to 650nm. Altering the composition of the core material can also change the emission wavelength. Thus, QDs have the benefit of being tuned to produce a vast array of fluorophores with the same material [35].

Typically, BRET sensors utilize fluorescent proteins [19,20,36–38] or organic dyes [39,40] as acceptors. However, recent studies report the use of nanoparticles such as quantum dots (QD) to be effective. QDs have the advantage of adjustable emission depending on size, superior brightness, high photostability, and multiplexing [41,42]. Fluorescent semiconductor quantum dots were previously limited in their application for *in vivo* imaging due to requiring excitation from an external source of light [20–23]. QDs can be excited by a broad range of wavelengths, from UV to the visible region. Therefore, they are able to be excited by virtually all bioluminescent proteins that are currently being used in BRET sensors [22]. In addition, their emission spectra are particularly narrow and tunable by size, thereby demonstrating excellent separation from the emission peak of bioluminescent proteins. QDs are also characterized by superior brightness and photostability, which are ideal traits for use as BRET acceptor molecules. QDs are also exceptionally resistant to photo and chemical degradation, feature large effective Stokes shifts, and boast high molar extinction coefficients that exceed organic dyes by 10-50 times [32]. Due to a high molar extinction coefficient, QDs can absorb 10-50 times more photons than organic dyes at the same excitation photon flux [43]. QDs are significantly more resistant to photobleaching, therefore, they are well-suited for continuous tracking studies over a long period of time [44]. Due to having a longer excited state lifetime, QDs will continue to emit light for long enough that background autofluorescence emission is over before QD emission ends [44]. The large Stokes shifts (measure of distance between excitation and emission peaks) of QDs can be used to improve detection sensitivity. Organic dyes with small Stokes shift are buried by strong tissue autofluorescence, whereas QD signals with large Stokes shift are easily detected above the background [42]. Tunable emission spectra are highly desirable for tracking multiple parameters such as in multiplexing. QDs are attractive in this regard because their broad absorption profiles allow simultaneous excitation of multiple colors [42].

Although not normally biocompatible, QDs can be modified through surface functionalization with hydrophilic ligands such as thiols, amine or carboxyls [45]. In addition to mediating solubility of the QDs, the ligands serve as a point of chemical attachment for biomolecules. For BRET sensors, these ligands can be utilized to conjugate the QDs to bioluminescent proteins or any such proteins [46].

When compared to organic dyes, multiple QDs are able to interact with a single BRET donor molecule. For example, for a single donor-dye acceptor pair, the FRET efficiency would be 22%. Increasing the number of acceptors to five increases the efficiency to 58% [32].

Cadmium telluride (CdTe) are well established and high-quality quantum dots which consists of II/VI semiconductors. The ability to synthesize CdTe with different capping ligands or encapsulated give them great potential for biological probes and optoelectronic devices [47]. Through the aqueous solution preparation method, QDs can be synthesized to be more biocompatible in addition to improved water stability [48,49].

1.5 Hypothesis

Bioluminescence resonance energy transfer is an ideal method for the detection and measuring of low concentration analytes such as glucose in tears. The challenge in the traditional BRET sensor design requires very narrow and specific BRET pairs. We propose the construction of a BRET-based biosensor using a BRET pair that is very flexible. In this novel BRET construct, the traditionally used BRET acceptor has been replaced with quantum dots. Cadmium tellurite quantum dots with an emission wavelength of 580nm will be conjugated to a glucose binding protein which is already conjugated to *Renilla* luciferase. *Renilla* luciferase will emit at 480nm in order to excite the quantum dots. The glucose binding protein will change conformation upon binding glucose and will bring the BRET pair closer together, thereby increasing the emission of the quantum dots.

1.6 Thesis objectives and motivation

Bioluminescence resonance energy transfer sensors offer a high degree of sensitivity and reliability in a procedure that is both easy to perform and relatively expensive. BRET sensors are more biocompatible and easier to perform modification of fluorescence resonance energy transfer which requires an external light source to initiate the fluorescence transfer. No longer requiring an external light source has made BRET attractive for use in biological systems, which may be susceptible

to tissue autofluorescence and photobleaching. Recent works have explored the potential of measuring other bodily fluids, which have a strong correlation to blood glucose levels.

BRET sensors utilizing a nanomaterial-based acceptor such as quantum dots have only been recently explored. Therefore, the motivation of this thesis is to explore the potential of a bioluminescent protein and quantum dot pair for use in a BRET sensor. In this study, the interaction between the two and how they can be effectively implemented into a BRET system will be investigated.

The objective of this thesis is to integrate inorganic nanomaterial and bioluminescence proteins into a non-invasive means of measuring blood glucose. The intent is to construct a BRET sensor utilizing quantum dots as the donor molecules and bioluminescent enzymes as the acceptor molecules and evaluate their performance *in vitro*. The proposed senor will use the luciferase from *Renilla reniformis* (emission wavelength λ_{cm} = 480nm) and incorporate it into a recombinant protein with glucose binding protein (GBP). The recombinant protein will be conjugated to CdTe quantum dots (emission wavelength λ_{cm} = 565nm).

The GBP acts as a separator of the donor and acceptor, keeping them at a distance from each other. Due to the distance dependent relationship of the donor-acceptor pair, the BRET emission will be weak [50]. However, when GBP binds glucose, it will change conformation, thereby shortening the distance between the donor-acceptor pair and increasing the BRET emission (Figure 1.2).

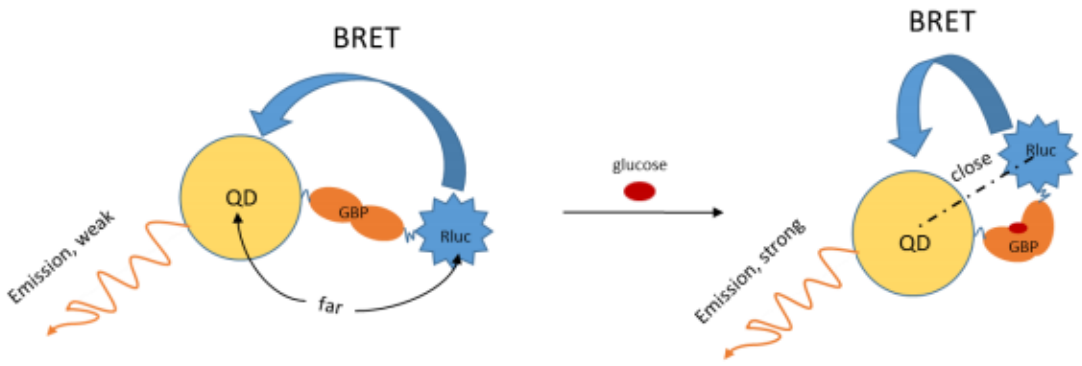

Figure 1.2: Schematic of the proposed BRET sensor. Quantum dots (QD) are used as the acceptor and *Renilla* luciferase (Rluc) as the donor. GBP separates the donor-acceptor pair and will change conformation upon binding glucose, thereby increasing the BRET emission intensity.

This study will lay the foundation for the use of inorganic nanomaterial in BRET sensors for the detection of small molecules relevant to human disease, particularly using quantum dots to offer an alternative and more sensitive means of monitoring concentrations of small molecules in the body. The following are sub-objectives in order to achieve the main objective:

- Synthesize and modify cadmium tellurite quantum dots with carboxylic groups in order to increase hydrophilicity and biological compatibility. Modifications enable the quantum dots to be conjugated to the protein
- Construct a recombinant plasmid containing the glucose binding protein, *Renilla luciferase* and His-tag protein, then transform into E. coli for rapid expansion. Extract and purify the target protein using a His-trap column.
- Bioconjugate the recombinant protein onto the CdTe
- Investigate optimizations of the construction of the sensor, particularly the protein to quantum dot ratio, the bioconjugation process, and concentration of glucose.
- Evaluate the performance of the biosensor when applied to a solid substrate.

1.7 Thesis overview

Chapter 2: Literature review

This chapter focuses on reviewing applications and techniques of biosensing, particularly involving quantum dots. In addition, techniques for glucose biosensing will be reviewed.

Chapter 3: Experimental methods

This chapter will describe the experimental procedures for synthesizing the different components of the biosensor. Procedures for synthesizing water-soluble cadmium tellurite quantum dots, construction of the recombinant plasmid, extraction and purification of the protein, conjugation of the protein and quantum dots are discussed in this section. In addition, characterization methods are discussed, such as the sodium dodecyl sulfate polyacrylamide gel electrophoresis (SDS-PAGE) and fluorescence emission spectra.

Chapter 4: Biosensor evaluation and optimization

The biosensor performance is evaluated. Optimization of the performance is evaluated through investigating changes in protein to quantum dot ratio, the bioconjugation process, and concentration of glucose present.

Chapter 5: Biosensor evaluation on solid substrate

Performance of the biosensor on a solid substrate is evaluated. The process by which the solid substrate is synthesized and also the conjugation process of the biosensor onto the substrate is discussed.

Chapter 6: Summary and future work

Conclusion and future of the sensor. Outlining how some aspects can be improved and its relevance compared to current work.

Chapter 2

2 Literature review

This chapter provides a literature review on the following aspects; (1) bioluminescence proteins in BRET sensors; (2) BRET phenomena and design; (3) quantum dots in BRET sensors. Different bioluminescent proteins are described based on their applicability in BRET sensors. In addition, the foundations and parameters for defining the BRET phenomena are described in detail. Then, BRET sensors utilizing quantum dots that have been previously developed are highlighted.

2.1 Bioluminescence proteins

FRET and, to an extent, BRET have typically utilized fluorescent proteins for both donor and acceptor molecules. Due to the need for external light to stimulate the fluorescent proteins, bioluminescent proteins have become increasingly attractive for use in resonance energy transfer-based sensors. Bioluminescent proteins do not require an external light source, only requiring a substrate, which is oxidized to produce light. Therefore, bioluminescent proteins have become more widespread in their use as reporters or donor molecules for BRET systems when measuring protein-protein interactions and small molecule concentrations[51].

There exists a variety of bioluminescence donors, many of which are derived from naturally occurring enzymes in animals such as the firefly or the sea pansy. Among the different donors, each has advantages and disadvantages in certain applications. Therefore, certain donors are considered for certain tasks according to their properties. This section aims to highlight some of the differences between bioluminescence donors and how they can be applied in BRET constructs.

Table 1: Summary of bioluminescent proteins

Name	Size (kDa)	Emission (nm)	Substrate
Aequorin	22	469	Coelenterazine
Bacterial luciferase (Lux)	α subunit: 40 β subunit: 35	490	$FMNH_2$ long-chain aliphatic aldehyde
Firefly luciferase (Fluc)	61	562	D-luciferin
Renilla luciferase (Rluc)	36	480	Coelenterazine
Gaussia luciferase (Gluc)	19.9	480	Coelenterazine
Vargula luciferase (Vluc) or *Cypridina* luciferase	62	460	Vargulin (*Cypridina* luciferin)
Metridia luciferase	24	480	Coelenterazine
Nano luciferase (Nluc)	19	460	Furimazine

2.1.1 Aequorin

First discovered in the jellyfish *Aequorea victoria*, aequorin is a 22 kDa photoprotein that emits blue light at 469 nm upon binding its substrate, coelenterazine [52,53]. Given its high sensitivity for calcium, aequorin is most often used to detect calcium concentration from a single cell by expressing it using recombinant aequorin [54–56]. Typically, aequorin is recombined with polyols to increase its stability [56]. Addition of coelenterazine to the medium allows it to passively diffuse into the cell, and aequorin emits blue light with intensity proportional to the calcium levels within the cell [53]. However, aequorin has a low light quantum yield compared to other bioluminescent proteins. Furthermore, its substrate, coelenterazine, has been shown to be unstable and have poor biodistribution [57].

2.1.2 Bacterial Luciferase

Bacterial luciferase (Lux) consists of two subunits: alpha, which is 40 kDa, and beta, which is 35 kDa; it emits blue light, which peaks at 490 nm [58,59]. Lux is an ATP-dependent luciferase and requires oxygen and NADPH as cofactors, in order to work on its substrate: long-chain aliphatic aldehydes and flavin mononucleotide ($FMNH_2$) [58,59]. It is most often used as a bacterial reporter, more specifically in luminous bacteria for autonomous bioluminescence oxidation reaction [59]. The long-chain aliphatic aldehydes have shown to be able to freely diffuse through the cell membrane and have high binding affinity for Lux [58]. Like aequorin, Lux demonstrates poor light quantum yield as well as poor thermostability [60]. Furthermore, studies are limited to luminous bacteria due to the cytotoxicity of aldehydes [61].

2.1.3 Firefly Luciferase

Firefly luciferase (Fluc), the first luciferase to be discovered, is a 61 kDa protein that emits blue light at 562 nm when exposed to its substrate, D-luciferin [62–64]. Similar to Lux, Fluc is ATP-dependent and requires the presence of co-factors, oxygen and magnesium, in order to complete its reaction with D-luciferin [63–65]. Since its discovery, Fluc has been used in various fields as a biosensor through recombination with another protein of interest and as ATP sensor, taking advantage of its ATP-dependency [66–68]. Fluc demonstrates high light quantum yield making it superior in comparison to Lux and aequorin [64]. Nonetheless, disadvantages involving Fluc as well as D-luciferin has emerged. Although D-luciferin had been presumed to have good biodistribution given its ability to cross the blood-brain barrier and blood-placental barrier, recent studies have discovered its low tissue permeability, which results in heterogenous biodistribution [57,69,70]. Furthermore, D-luciferin has low affinity for Fluc, which may result in false negative signals [57]. Moreover, Fluc and D-luciferin only gives a single imaging signal limiting studies to a single molecular event or a single population of cells [57]. Finally, the large size of Fluc may lead to steric hindrance when used as a recombinant protein [65].

2.1.4 *Renilla* Luciferase

Renilla luciferase (Rluc), first discovered in sea pansy, *Renilla reniformis*, is a 36 kDa protein that emits blue light at 480 nm when worked with its substrate, coelenterazine [71–73]. Rluc is often used as a marker for gene expression in mammalian cells and as a biosensor when recombined with a protein of interest [72,74]. As it originates from non-mammalian cells, the gene sequence for Rluc includes codons that are uncommon in mammalian cells, which limits Rluc expression in the cells [71]. Furthermore, Rluc has shown to have low enzymatic turnover and quantum yield when compared to Fluc [73,75]. In addition, the problem of instability and poor biodistribution of coelenterazine remains [57].

2.1.5 *Gaussia* Luciferase

Gaussia luciferase (Gluc) is similar to Rluc due to having an emission peak at 480 nm, ATP-independence, and bind the same substrate, coelenterazine [65,73,75]. Gluc is smaller than Rluc at 19.9 kDa and originates from *Gaussia princeps*, thus eliminating the problem of uncommon codons [75]. Gluc has been used as a bioluminescent label for in vitro hybridization assay as well as a biosensor through recombination with another protein of interest [65,76]. Gluc is naturally secreted by the cells, which allows for it to be detectable in cell medium [75,77]. It has also been characterized to be more sensitive compared to Fluc and Rluc [77]. Despite its sensitivity, quantum yield remains low and is accompanied by problems involving coelenterazine [57,73,78].

2.1.6 *Vargula* Luciferase

Vargula luciferase (Vluc), also known as *Cypridina* luciferase, is a 62 kDa protein that emits blue light at 460 nm when worked with its substrate, vargulin, also known as *cypridina* luciferin [79–81]. Similar to Rluc, Vluc has been used as a marker for gene expression in mammalian cells as well as a biosensor when recombined with another protein of interest [80,82]. Also, similar to Gluc, Vluc is also naturally secreted by cells, and it is detectable in cell medium [82]. One advantage of Vluc over other luciferases is its glow-type bioluminescence compared to flash-type exhibited by other luciferases [81]. Previously, Vluc has been shown to be difficult to express and purify from bacterial

systems; however, the issue has been successfully addressed by using a truncated derivative of Vluc, which shows higher degree of expression and purification while retaining its enzymatic activity [81].

2.1.7 Metridia Luciferase

Like Rluc and Gluc, *Metridia* luciferase also emits blue light at 480 nm, is ATP-independent, and works on the same substrate, coelenterazine [73,76,83]. Smaller than Gluc but bigger than Rluc, *Metridia* luciferase is 24 kDa protein [83]. Similar to all luciferase, *Metridia* luciferase has been used as a biosensor by recombining it with another protein of interest [83]. *Metridia* luciferase is also naturally secreted by cells similar to Vluc and Gluc [76]. In addition, its low molecular mass serves as an advantage in recombination [83]. However, *Metridia* luciferase demonstrates low quantum yield, and the disadvantages of coelenterazine discussed before stays relevant [57,73].

2.1.8 Nano Luciferase

Nano Luciferase (Nluc) is a recently developed luciferase that uses furimazine as a substrate to emit blue light at 460 nm [84–86]. It is the one of the smallest luciferases to be characterized at 19 kDa and has the one of the brightest bioluminescence to date [84,86]. Not many studies using Nluc has been published compared to other bioluminescent proteins as the molecule is fairly new; the published studies typically use Nluc as a biosensor through recombination with their protein of interest [86,87]. Nluc exhibits glow type bioluminescence, similar to Vluc, with long half-life of approximately 2 hours [84,86]. Furthermore, furimazine has shown to exhibit lower background noise when compared to coelenterazine.

2.2 BRET phenomena/design

Originally observed in marine animals, such as the sea pansy *Renilla reniformis*, BRET is a nonradiative energy transfer from a bioluminescent donor to a fluorescent acceptor. While the acceptor has traditionally employed the use of yellow fluorescent protein (YFP) when paired with Rluc, recent research has investigated the use of quantum dots as a suitable replacement for YFP [22,42,44,47,89–92]. When the donor is in close proximity

to the acceptor, the energy that results from catalytic degradation of a substrate, such as CTZ, is transferred from the donor to the acceptor, therefore inducing two light emissions. One light emission at 480nm corresponds to the donor and in the case of YFP, the second emission at 530nm corresponds to the acceptor. Therefore, the presence of both emissions indicates the coexpression of the donor and acceptor in close proximity [93].

The transfer of energy from donor to acceptor is only able to take place within 1-10nm which is also the distance for protein-protein interactions in the physiological environment. Therefore, observing a BRET signal indicates that in a system placed to monitor protein-protein interactions, such an interaction has occurred [94]. The design of the BRET partners should meet the following requirements: (1) the distance between the donor-acceptor pair should be less than 10 nm; (2) there should be spectral overlap between the donor emission and the acceptor excitation wavelengths; (3) the dipoles of the donor and acceptor should be aligned in order to maximize transfer of resonance energy through nonradiative dipole-dipole coupling; and (4) higher donor quantum output results in increased energy transfer to the acceptor therefore the donor quantum output should be greater than the energy loss due to decay [94–97].

Photoluminescent QDs are rapidly becoming popular choices for use in biomedical applications such as labeling, bioimaging, and biosensing. QDs are particularly appealing due to their high photostability, continuous absorption spectra, and size-dependent fluorescence [98–102]. QDs are typically synthesized as hydrophobic and therefore require a number of modifications in order to be suitable in biological environments. Modifying QDs to be suitable for solubility in water results in a decreased quantum yield and therefore requires surface modifications [88,103]. There exist three strategies to make QDs water soluble: ligand exchange, silanization, and encapsulation.

In ligand exchange, the original hydrophobic coating is replaced by a water-soluble bifunctional molecule. Once attached to the QD surface, a hydrophilic tail makes the QDs able to bioconjugate, usually with other surface groups such as thiol, amine and carboxyl [104].

Silanization is an extension of ligand exchange where the QD is coated in a silica shell, which is non-toxic, chemically inert and optically transparent. The silica shell protects the QD from oxidization and provides a matrix, which enhances stability in the environment. The silica is biocompatible and can be functionalized for bioconjugation [105–107].

Encapsulation utilizes different carriers such as amphiphilic polymers, polymeric microbeads, and liposomes [108–110]. These coating molecules have hydrophobic and hydrophilic units, therefore can interact strongly with the QD surface and the aqueous outside environment [108]. Liposomes are particularly popular due to their porous spherical structure and high loading capacity [109,111]. However, they are limited due to susceptibility to temperature and pH changes [112].

There are two primary approaches to bind biomolecules onto the surface of QDs. Non-covalent which is mediated by interactions between the biomolecules and the QD surface, and covalent linking which is achieved through chemical reactions of molecular surface groups [110,113].

Non-covalent binding is achieved through two types of interactions; electrostatic interaction between oppositely charged molecules and high affinity secondary interactions. QDs are negatively charged on the surface, therefore can be electrostatically coupled to positively charged proteins [110,114]. High affinity secondary interactions are interactions between functional groups on the surface of the QD and the biomolecule. Biotin-avidin is a commonly utilized combination, though limited by the increased size of the product [114,115]. The interaction between His-tagged biomolecules and Ni-NTA is widely used in bioconjugation and often used for developing a QD probe for performing Western blot analyses [114,115].

Covalent binding involves the reaction between functional groups on QDs and biomolecules. Crosslinkers can be used to bind the molecules. Zero-length crosslinkers such as 1-ethyl-3-(3-dimethylami-nopropyl) carbodiimide (EDC) are used because they will not add any more atoms [116]. Carboxylic functionalized QDs are among the most popular due to the abundance of free amine groups on proteins, which they can conjugate

with [117]. The most popular method utilizes EDC which mediates the formation of an amide bond between the carboxyl on QDs and amines on biomolecules [116,118].

Quantum dots cores consist of various metal complexes which have raised questions about their application in a biological setting [119]. This concern is commonly resolved by adding organic coatings such as methoxy-polyethylene glycol (PEG) to the surface in order to increase biocompatibility [120]. Commonly used quantum dots include CdTe and CdSe and all of these metals are known to be toxic to humans when exposed upon degradation of the quantum dots [121–124]. There is lack of biocompatibility data for quantum dots and little research done on the effect on humans. Part of the reason can be attributed to the various factors related to physicochemical properties of quantum dots like size, charge, concentration, outer coating and mechanical stability [125,126]. Various studies have found adverse effects due to quantum dots [127] and some have found little to no adverse effects, given some modifications [128,129]. Studies have determined that quantum dots have a significantly long half-life and the degradation of fluorescent particles taking almost 12 weeks in the liver [120,130]. This uncertainty in terms of biocompatibility warrants further investigation, particularly in human subjects.

2.3 Quantum dots in BRET sensors

Quantum dots have been reported for their distinct advantages when used as acceptors in BRET sensors. Quantum dots have the distinct advantage of an adjustable emission based on their size, which can be controlled during their synthesis. In one particular study, the emission of the quantum dots could be adjusted by adjusting the feeding ratio of indium/zinc [46]. By increasing the amount of indium compared to zinc, the emission wavelength could be increased (Figure 2.1). The quantum dot emission can also be adjusted by varying the refluxing period during synthesis. Tunable emissions are particularly attractive for BRET sensors because the flexibility of the quantum dots allows them to be paired with a variety of bioluminescent proteins. Different types of bioluminescent proteins have varying emission wavelengths; therefore, it is advantageous for quantum dots to adjust their emissions in order to align with the protein emission.

QDs have been used with a variety of donor molecules such as Rluc [22,131,132], Fluc [51,133], and Nluc [134] for developing biosensors and biomarker assays in addition to *in vitro* and *in vivo* imaging [132].

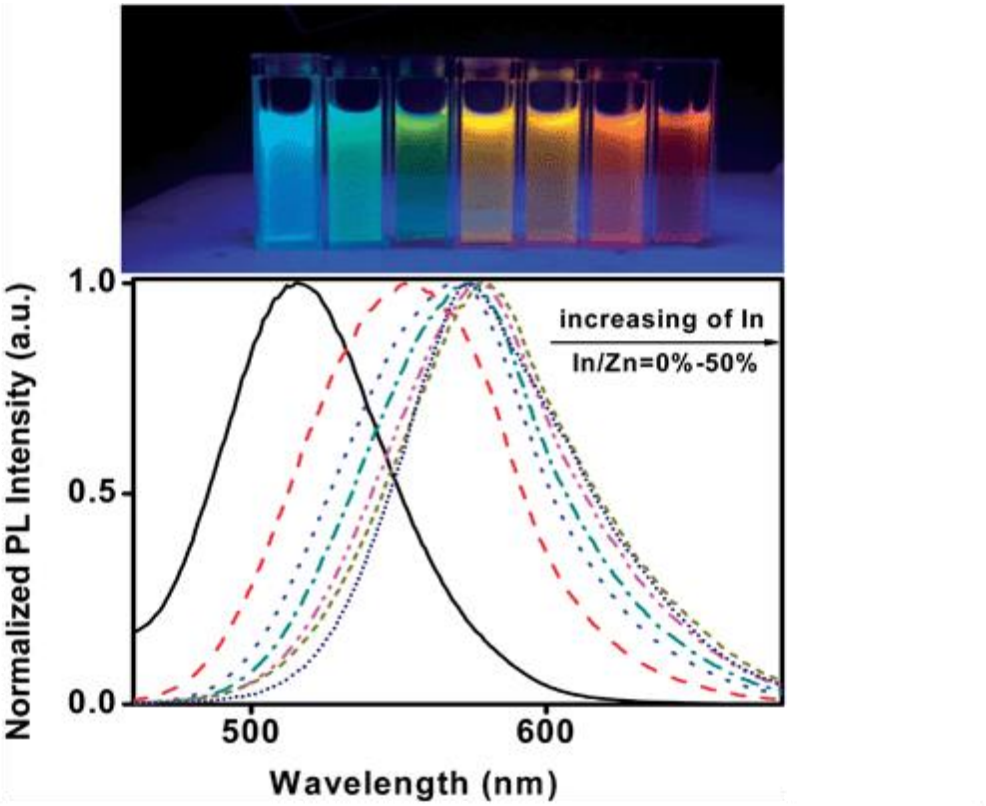

Figure 2.1: Photoluminescence spectra under irradiation of a UV lamp (12 W, 365nm) of Ag:ZnInSe QDs at different In/Zn feeding ratios 0-50% from left to right. All samples are left to react for 4h. Reprinted (adapted) with permission from [46]**. Copyright 2000 American Chemical Society.**

2.3.1 Quantum dot-based BRET sensors for detecting biomolecules

Carboxylated quantum dots (Qd-625) were conjugated to a DNA probe (Qd-D-P) while oligonucleotide probes were conjugated to Rluc (Rluc-P). The sensing scheme uses the two antisense oligonucleotide sequences which will anneal adjacent to each other in a head-to-head fashion when the target is present (Figure 2.2) The maximum BRET signal was obtained by optimizing the spacing between the Rluc-P and Qd-D-P when hybridized to the target. Optimization was done using oligonucleotide targets, which create various

separation distances. The optimal separation distance was found to be 15 nucleotides. Hybridization time between labeled probes and target was studied and found the optimal time to be 5 and 35 minutes. In conclusion, an on-type, BRET-based sensing platform incorporating Rluc and QD with a 5-minute detection time of a nucleic acid target *in vitro* was developed. The method was also determined to be highly sensitive (detection limit of 0.54 pmol) and selective against mismatch targets [135].

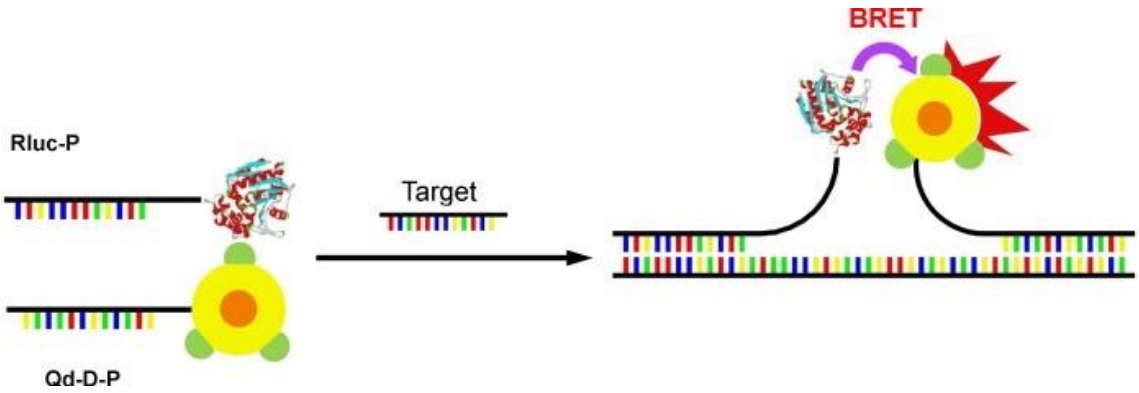

Figure 2.2: Schematic of BRET based on-type sensing system. The Rluc-P and Qd-D-P hybridized to the target in head-to-head fashion permitting BRET between Rluc and Qd. Reprinted from [135], with permission from Elsevier

Near-infrared region optical detection of apoptotic cells was achieved using BRET-coupled annexin V-functionalized quantum dots. A recombinant protein with Rluc and annexin V was conjugated to glutathione coated CdSeTe/CdS QDs (Figure 2.3A). Annexin V recognizes phosphatidylserine (PS) on the outer monolayer of the membrane of apoptotic cells and binds to it in the presence of Ca^{2+} ions (Figure 2.3B). The QDs act as a probe for detecting apoptotic cells with a peak emission at 830 nm and a high quantum yield of 61% in aqueous solution. This method was presented as a simple, rapid, and efficient method for synthesizing a BRET-induced NIR emission probe and with its low phototoxicity could prove to be useful in highly sensitive detection of apoptotic cells *in vivo* and *in vitro* [136].

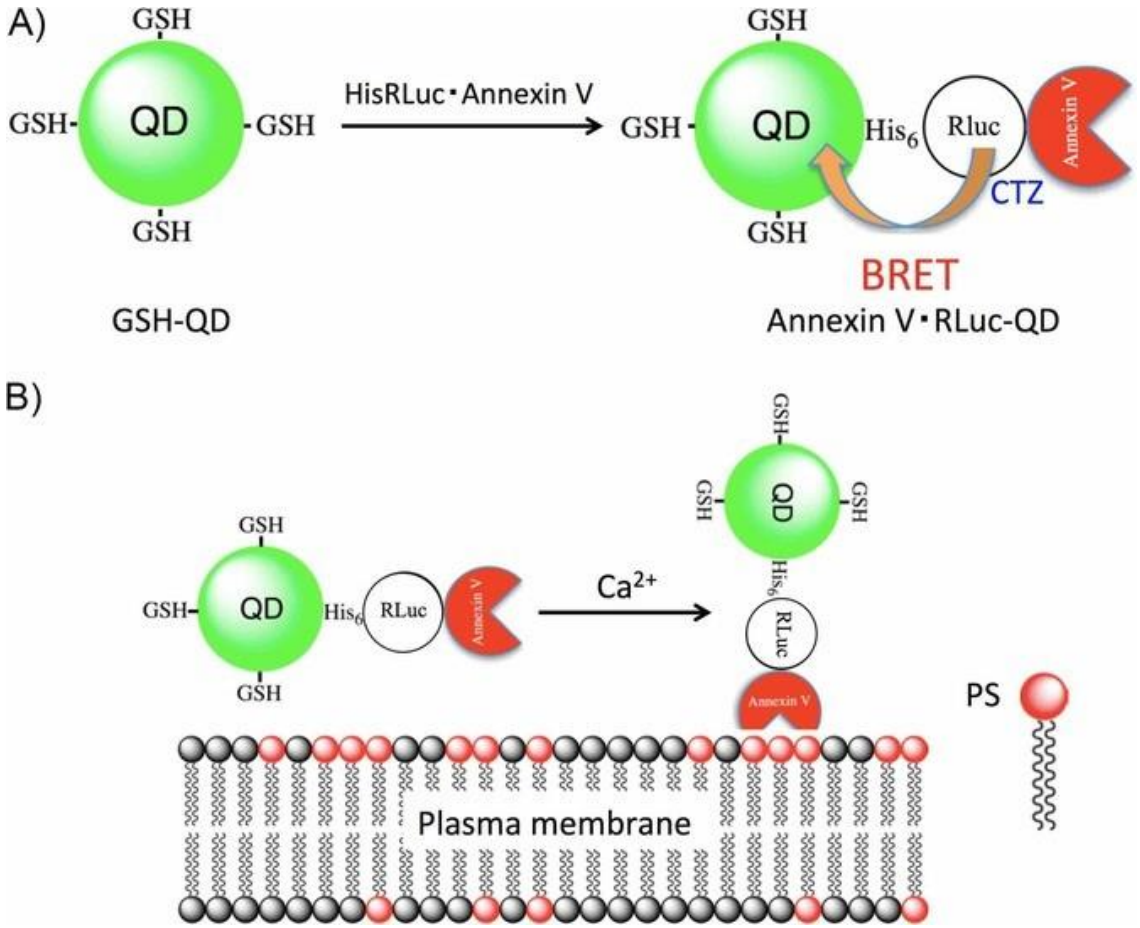

Figure 2.3: A) Synthetic method for the preparation of recombinant protein (HisRLuc-annexin V)-conjugated QDs (annexin V-Rluc-QDs). B) Schematic representation for the binding of annexin V-RLuc-QDs to PS on plasma membrane of apoptotic cells in the presence of Ca^{2+} ions. Reprinted with permission from [136]. Copyright 2017 John Wiley and Sons

A general BRET homogenous immunoassay was developed for the determination of small molecules. This assay is based on QDs and Rluc which produce variable energy transfer in the presence of different concentrations of free fluoroquinolones (FQs). In the absence of free FQs, QDs conjugated to norfloxacin (QD-NOR) are recognized by a single-chain variable fragment (scFv), which is conjugated to Rluc, and are able to produce an energy transfer (Figure 2.4A). Otherwise, the presence of Free FQs prevents the Rluc and QDs from producing and energy transfer (Figure 2.4B). Similar results for cross-reactivity to seven representative FQs were found when compared to an enzyme-

linked immunosorbent assay (ELISA). The LOD of the QD-BRET immunoassay was 2.54 ng/L with a linear range which covers 4 orders of magnitude (0.023 to 25.60 ng/ml). The use of QDs enables the flexibility of more choices for donor substrates given the wider excitation range of the QDs. The authors noted that by replacing the target of interest, the immunosensor could be used with a variety of other small molecules and could open up the possibility of multiplex detection using different QDs [92].

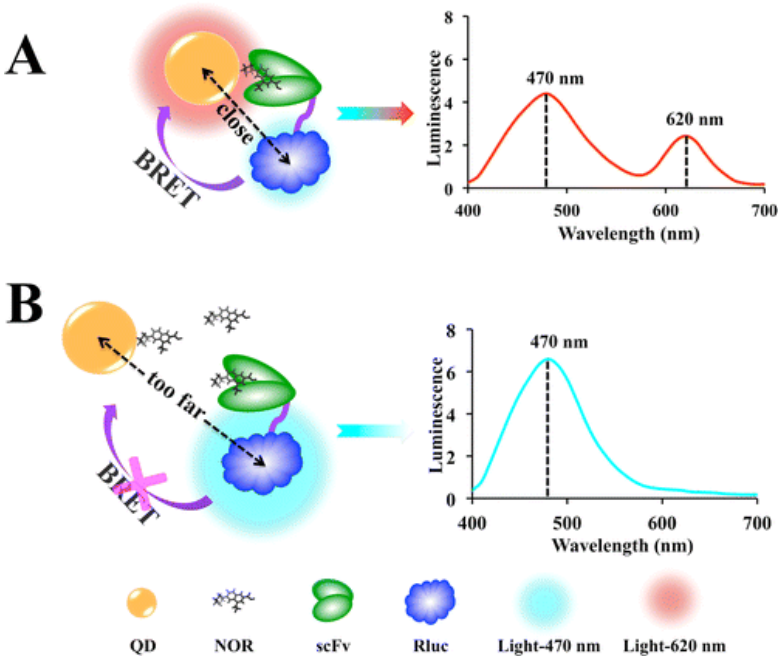

Figure 2.4: A) In the absence of free FQs, QD-NOR is recognized by scFv-Rluc and the Rluc and QDs are in close proximity; energy is released from the substrate and transferred to the QDs via BRET. B) In the presence of free FQs, the scFv-Rluc binds to the free FQs and the distance between the Rluc and QDs is too far to realize energy transfer. Reprinted (adapted) with permission from [126]. Copyright 2016 American Chemical Society.

In one particular study, CdSe/ZnS core-shell quantum dots (QD705) were conjugated to Nluc (Figure 2.5). This construct was used to image tumors by conjugating it to cyclic arginine-glycine-aspartic acid (cRGD) peptides, which were selected due to having strong affinity for integrin $\alpha_v\beta_3$, which are known to be expressed on various tumor types. When intradermally injected into the hind paw of a mouse, the popliteal lymph nodes could be visualized by bioluminescence at 5 minutes post injection (p.i.) without any background signal. To demonstrate tumor-targeting capabilities, the sensor was injected into mice with integrin expressing U87MG human glioblastoma cell tumors. After 2 hours, p.i. organs were harvested and *ex vivo* imaging found a noticeably visible signal in the tumors injected with QD-Nluc-cRGD. When compared to traditional fluorescence techniques, bioluminescence demonstrated higher sensitivity due to the distance dependent relationship of BRET components. Using the BRET conjugate, the tumor to background ratio was exceptionally high (>85) [134].

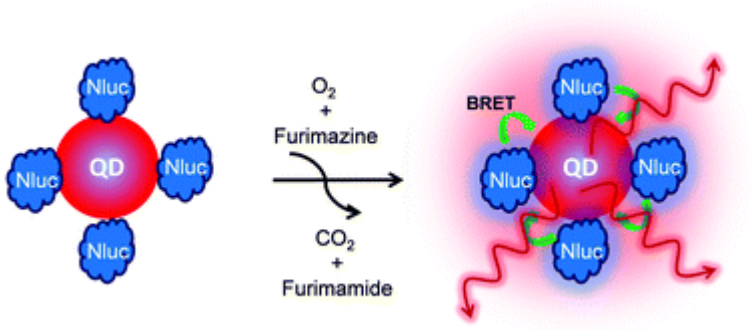

Figure 2.5: QD-Nluc-cRGD conjugate. Chemical communications by Royal Soceity of Chemistry (Great Britain). Reproduced with permission of ROYAL SOCIETY OF CHEMISTRY.

2.3.2 QD-based BRET sensor used in bioimaging *in vivo*

BRET-QD nanoparticles were applied to *in vivo* lymphatic imaging in mice. QD655 covalently linked to Luc8 protein, an eight-mutation variant of Rluc, were intracutaneously injected into 10 weak old normal athymic female mice at different sites, the chin, ear and paws. After 5 minutes, the imaging was carried out (Figure 2.6). Using BRET-QD655 has the advantage over traditional bioluminescence imaging (BLI) in that NIR light emission is more favorable in tissue penetration. All lymph nodes

were visualized when injected with BRET-QD655 constructs and since there is no excitation light, the BRET signal more accurately represents the concentration of the quantum dots in the lymph nodes, leading to better quantitative imaging [137].

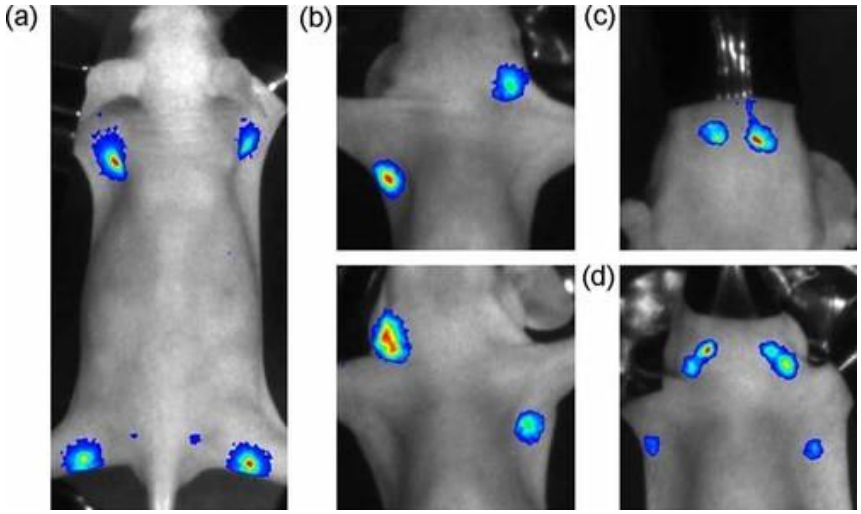

Figure 2.6: BRET lymphatic images of different lymphatic basins. BRET-QD655 were injected at all four paws (a), the ear and forepaw (b), the chin (c), or five different sites (d: both forepaws, both ears and chin). Copyright 2011 John Wiley and Sons

The use of QD nanoparticles as a tool for non-invasive investigation of mammalian spermatozoa was explored. CdSe/ZnS QD nanoparticles with emission wavelengths of 655 nm were conjugated to nona-Arginine R9 peptide, which facilitates cellular internalization. The QDs were linked to RLuc and used to label boar spermatozoa and were assessed for changes in sperm motility, viability, and fertilizing potential. *In vitro* assays concluded no adverse effect of the BRET-QD on the spermatozoa. The results suggest the strong potential for a novel imaging technique for tracking BRET-QD labeled spermatozoa to better understand sperm migration within the female genital tract [138].

BRET coupled near infrared quantum dots were used as a highly sensitive near-infrared optical detector of epidermal growth factor receptors expressed on cancer cells. His-tagged Rluc recombinant protein (HisRluc·GB1) were conjugated to glutathione-coated CdSeTe/CdS QDs (GSH-QDs) to form conjugated QDs (GB1·Rluc-QDs). The

recombinant protein consists of a luciferase enzyme and immunoglobulin-binding domain (GB1) of protein G. The GB1 domain allows the GB1·Rluc-QDs to bind the Fc moiety of immunoglobulin G which is then used as a molecular imaging probe using NIR fluorescence and BRET-coupled NIR emission. In order to detect EGFRs on cancer cells, anti-EGFR monoclonal antibodies were conjugated to the GB1·Rluc-QDs (Figure 2.7). The detection sensitivity of EDGRs by BRET-coupled NIR emission of the GB1·Rluc-QDs was found to be over three times higher than NIR fluorescence of the QDs. Therefore the conjugation of the antibody with GB1·Rluc-QDs have proven successful in performing BRET-based highly sensitive NIR imaging of EGDRs in living cells [91].

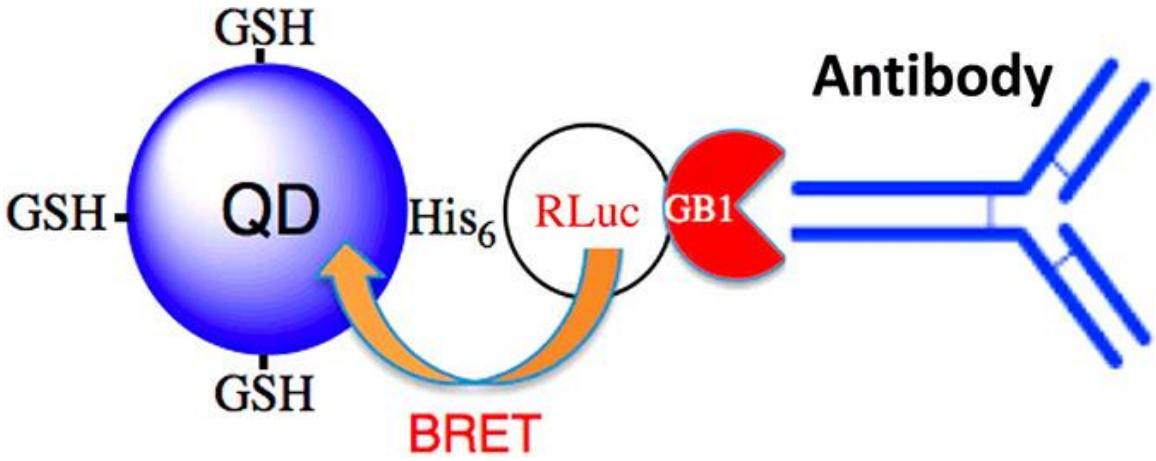

Figure 2.7. Prepared BRET-coupled NIR-QDs (GB1·Rluc-QDs) using glutathione-capped QDs (GSH-QD). BRET-coupled NIR emission from antibody conjugates with GB1·Rluc-QDs occurs in the presence of coelenterazine (CTZ). Reprinted (adapted) with permission from [129]. Copyright 2018 American Chemical Society.

Chapter 3

3 Experimental methods

3.1 Recombinant plasmid construction

The recombinant plasmid was constructed using the *mglb* gene from *E. coli* k-12 connected by a six amino acid linker to the *Rluc* gene cloned from the plasmid pRL-null (Promega, Inc). These encode for wild-type glucose binding protein (GBP) and *Renilla* luciferase, respectively. Primers for GBP were designed for cloning (forward 5' TATACATATGAATAAGAAGGTGTTAACCCTGTCTGC 3'; reverse 5' GCTGGATCCTTTCTTGCTGAATTCAGCCAGGTTG 3'). These primers were introduced at the restriction site Nde I and BamH I, respectively. A six amino acid linker SGGGGS was inserted after the BamH I site in order to separate the GBP and Rluc. The primers for Rluc are also follows: (forward 5' AAAGGATCCAGCGGTGGTGGTGGTAGCATGACTTCGAAAGTTTATGATCCAG 3'; reverse 5' TGTGCTCGAGTTGTTCATTTTT GAGAACTCGCTC 3'). The reverse primer for Rluc was introduced at the restriction site Xho I. Therefore, the GBP gene is located upstream of the fusion protein.

The PCR products were digested with their related restriction enzyme and the plasmid pET32a (Novagen, Inc) was used to clone and express the recombinant gene. The digested DNA inserts were ligated into the related MCS (multiple cloning site) in pET32a. A six-histidine tail was added to the GBP-Rluc recombinant protein for use in purifying the protein. The pET32a-GBP-Rluc plasmid was transformed into *E. coli* BL21 cells for rapid expansion. The DNA sequence of the recombinant plasmid was confirmed by DNA sequencing (Robarts Research Institute, Western University).

3.2 Recombinant protein extraction and purification

3.2.1 Bacterial culture

The bacteria were cultured on an agar plate until colonies were visible. A 5 mL starter culture of Luria-Betrani (LB) broth containing 100 µg/mL ampicillin was inoculated with the bacteria and grown overnight at 37°C. The culture was then used to inoculate 800 mL

of LB broth containing 100 µg/mL and left to grow at 37°C. When the culture achieved an OD600 of 0.375, isopropyl β-D-1-thiogalactopyranoside (IPTG) was added to the culture to a final concentration of 1mM in order to induce expression of GBP-Rluc. The culture was then left to grow for four hours at 21°C on a shaker at 200RPM.

3.2.2 Protein extraction and purification

The bacteria culture was centrifuged at 9 000 RPM for 5 minutes at 4°C. The supernatant was discarded and the pellet was suspended in binding solution, which is comprised of 20mM Tris/HCl, 500mM NaCl, 5mM imidazole at pH 7.4. The solution was then sonicated on ice using 15-second bursts followed by 30 seconds of rest for 30 cycles using a Mandel Scientific Q500 sonicator.

The solution was then centrifuged at 8 000 RPM at 4°C for 30 minutes. The supernatant was collected and filtered using a cellulose acetate membrane syringe filter (VWR, Inc.) with a pore size of 0.45µm.

The protein solution was purified using His-trap HP columns (GE Lifesciences. Inc.) by a syringe pump. The column is equilibrated using binding solution and the supernatant is loaded into the column at a rate of 0.3mL/min. The column is washed with 10 column volumes of binding solution afterwards. In order to elute the protein from the column, and increasing gradient of imidazole is used to wash out the column. The concentrations of imidazole used are as follows: 40mM, 60mM, 80mM, and 120mM. Each concentration of imidazole is used at 10 column volumes at a rate of 0.5mL/min to wash the column starting from the lowest concentration. The imidazole used to wash out the column were then collected in order to be used to identify the concentration in which the protein was eluted.

The gradient of concentrations was run in sodium dodecyl sulfate polyacrylamide gel electrophoresis (10% SDS-PAGE) in order to verify that the target protein was purified and the relative concentration in each solution. Samples were prepared in 1:1 solution with SDS running buffer and boiled for 5 minutes. The samples were run alongside PageRuler^{TM} Prestained Protein Ladder (ThermoFischer Scientific). The gel was run at 120V for 34

minutes, then stained using Coomassie Blue for 40 minutes. Destaining took place overnight using distilled water.

Upon verification of the presence of purified protein in each of the imidazole samples, the solutions were concentrated using an Amicon Ultra centrifugal filter (ultra-15, MWCO 10kDa, Millipore Inc.) and collected in one tube. The concentration of the protein was determined by bicinchoninic acid assay (BCA) using bovine serum albumin as the standard. The concentration was then adjusted to the desired amount by either centrifuging to a lower volume or increasing the volume.

3.3 Cadmium tellurite quantum dot synthesis

Cadmium tellurite quantum dots (CdTe QDs) were prepared using a one-pot synthesis method [139]. In a three-necked flask, 0.4mmol $Cd(CH_3COO)_2 \cdot 2H_2O$ was dissolved in 60 mL of deionized water. After 10 minutes, 36µL TGA was added into the solution and stirred for 5 minutes. Then 0.08mmol Na_2TeO_3 was dissolved in 50mL of deionized water and added to the above solution. After 3 minutes of stirring, 160 mg of $NaBH_4$ was added to the solution and the pH was adjusted to 11 using 1M NaOH. The solution was refluxed at 100°C with a condenser under open-air conditions. The desired photoluminescent emission spectra was acquired by controlling the reaction time. In order to achieve the spectra required for this particular project, the reaction was ended at 2 hours. The quantum dots were then washed twice with ethanol and dissolved in deionized water.

3.4 Protein and quantum dot bioconjugation

Bioconjugation was mediated by 1-ethyl-3-(3-dimethylami-nopropyl) carbodiimide (EDC). Varying ratios of the TGA stabilized CdTe, EDC and protein were used in order to determine the most ideal amounts of each. The total reaction time was also varied. The baseline ratios used are as follows: 10 µL of 2µmol/L CdTe, 10 µL of 20mmol/L EDC and 50 µL of 0.1 mmol/L recombinant protein in 80µL PBS. After the conclusion of the reaction, Amicon Ultra centrifugal filters (MWCO 100kDa, Millipore Inc.) were used to remove free particles from the solution.

3.5 Solid substrate synthesis

A well-aligned zinc oxide (ZnO) nanorod array was grown on PDMS film. 0.01M zinc acetate dehydrate was dissolved in 100 mL ethanol as a seed solution. The seed solution was dropped on a PDMS substrate repeatedly followed by heat treatment at 100°C for 1 hour. The film was ten immersed in a mixed solution of 0.025M zinc nitrate hexahydrate and 0.025M hexamethylenetetramine in 200 mL of distilled water. After 3 hours of heating at 90°C, the ZnO nanorod array was grown on the PDMS (Figure 5.1) [140].

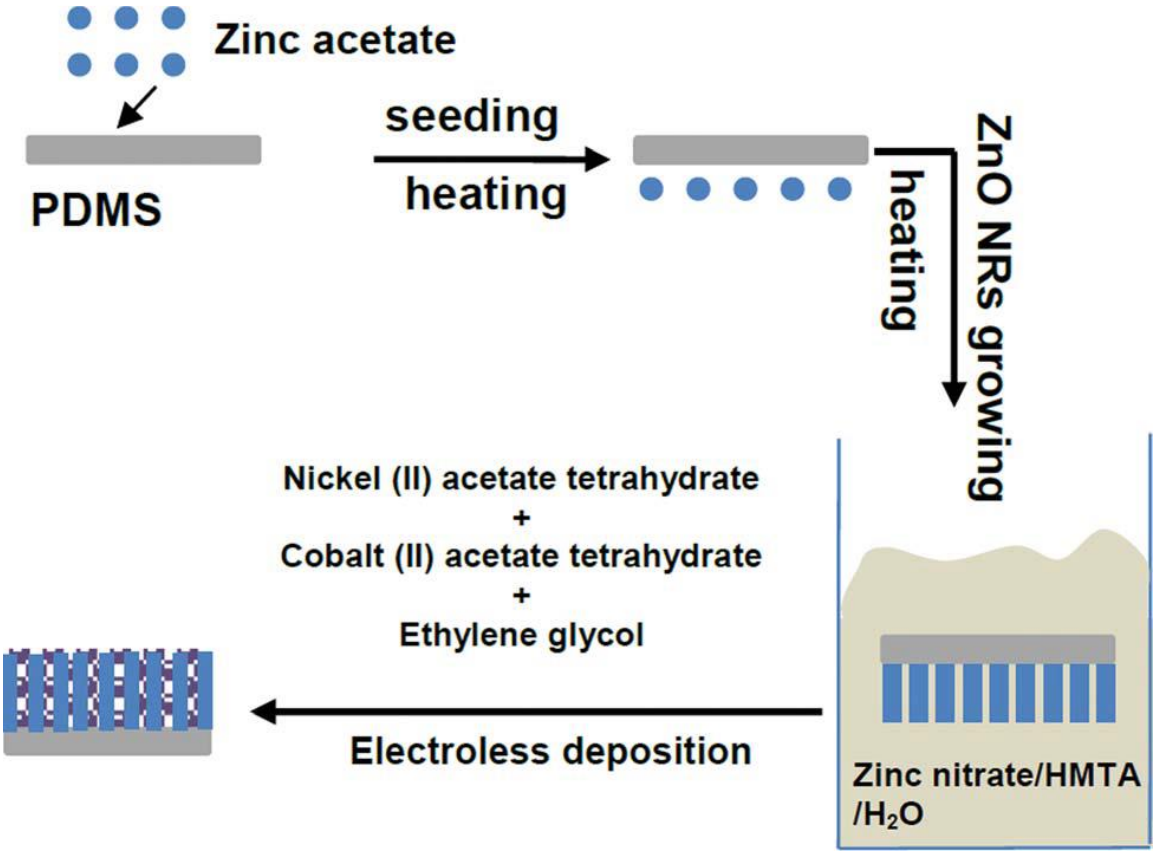

Figure 3.1: Illustration of the two-step method for fabricating nanocomposite coated ZnO nanorod array on PDMS

3.6 Conjugation of sensor onto substrate

CdTe QDs were conjugated to the ZnO nanoarray using EDC at a ratio of 10 000 to 1 QD. The substrate was then washed to remove all free particles and leftover EDC. The protein was then separately conjugated to the CdTe also using EDC at a ratio of 10 000 to 1 QD. The sample was incubated for 1 hour, then washed of any residual particles. 5µL of 1mM CTZ was added to the substrate and measured in the fluorescence spectrophotometer immediately. Unless otherwise stated, all samples were incubated with 3µL of 2µM of glucose solution for 5 minutes prior to the addition of CTZ.

3.7 Bioluminescence measurement

Measurement of the BRET signal of the biosensor was done after the sample was incubated with 2µM of 10mM glucose for 5 minutes. Then 5µM of 1mM CTZ was added to the sensor solution immediately before initiating the fluorescence spectrophotometer. The spectrophotometer was set to read fluorescence intensity every 10 nm of wavelength with a time of 0.5 seconds between each reading. Due to the concentration of protein required, each test was repeated two or three times and the best representation was selected to be presented.

3.8 Characterization methods

Molar concentration of the quantum dot solutions was calculated using UV-vis spectrometry. The determination of the concentration relies on Beer's Law using the extinction coefficient ε (10^5 cm^{-1} M^{-1}). For CdTe, ε = 10043 $(D)^{2.12}$, where D is the diameter of the quantum dots (nm). Using Beer's Law, the concentration can be calculated using equation (2):

$$\lambda = \varepsilon * C * L \tag{2}$$

Where C is the concentration of QDs in mol/L, and L is the path length (cm) [141].

The concentration of the GBP-Rluc protein in solution was determined using a Micro BCA™ Protein Assay Kit (ThermoFisher Scientific). The solution concentration was then adjusted to the desired concentration using 10mM PBS.

Chapter 4

4 Homogenous biosensor evaluation and optimization

4.1 Characterization

Verification of the extraction of the purified protein was completed through SDS-PAGE. Rluc and GBP are ~36kDa and ~33kDa respectively. Taking into account the 6x His-tag and linker, the predicted molecular weight of the recombinant protein is ~71kDa. SDS-PAGE performed on the protein solution purified through the His-trap HP columns revealed ~71kDa bands, thereby confirming the success of the purification process (Figure 3.1).

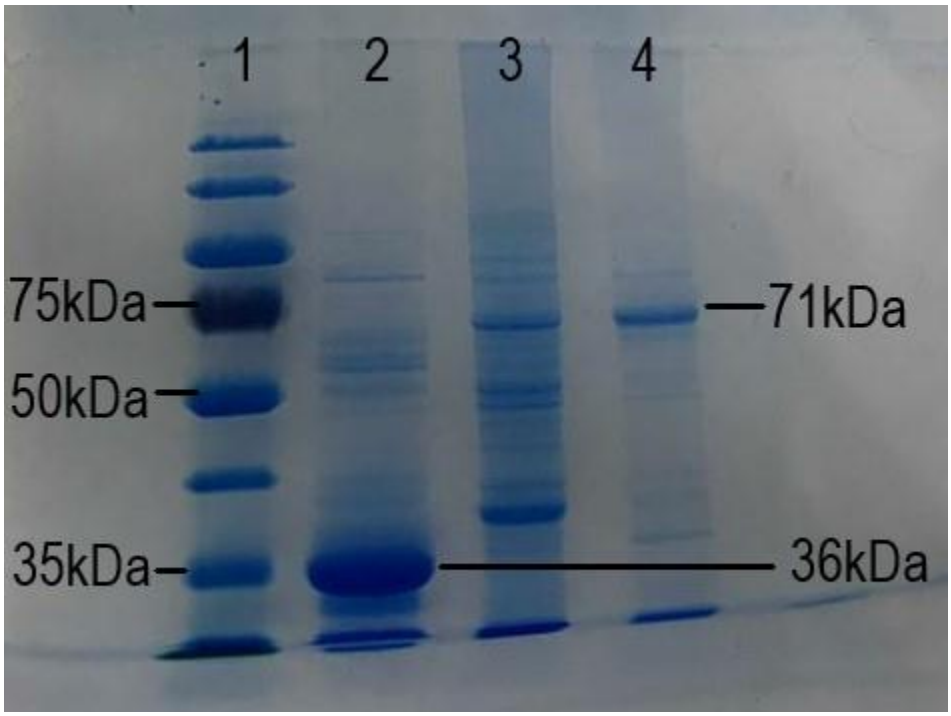

Figure 4.1: SDS-PAGE characterization of the recombinant protein, GBP-Rluc purified through His-trap HP columns. 1) PageRuler™ Prestained Protein Ladder. 2) Rluc only (~36kDa), 3) Unpurified protein sample, 4) Purified recombinant protein sample (~71kDa)

TEM imaging of the CdTe QDs determined the average particle size to be 10 ± 3nm (Appendix, Figure 1). Photoluminescence with an excitation wavelength of 480nm determined that the CdTe emission peak is centered at 580nm

4.2 Protein to quantum dot ratio

During the bioconjugation process, the ratio of the protein and quantum dots were varied in order to determine the ideal ratio. The most ideal ratio will ideally allow both the luciferase and QDs to show strong emission peaks in the emission spectra. The luciferase emission peak would be observed near 480nm and the quantum dot emission peak would be observed near the 580nm region. When synthesizing the quantum dots, the emission peak was carefully set by setting the time of refluxing to 2 hours. The emission peak of the quantum dots and luciferase were then verified individually using the fluorescence spectrophotometer. Due to initial findings indicating the protein emission being significantly higher than the QD, the ratio of QD was significantly increased.

GBP-Rluc purified from *E. coli* was conjugated to QDs synthesized using a one-pot synthesis method. EDC was used at a molar ratio of 100 EDC to 1 QD and allowed to conjugated for 1 hour. Results indicate a significant decrease in the intensity of the bioluminescence emitted by the Rluc with increasing concentrations of QDs. No discernible peak is observed for the luminescence emitted by the quantum dots despite significant increases in the ratio of QDs to protein. This is due to the high intensity of the bioluminescence masking the quantum dot emission. Therefore, the amount of bioluminescent protein was reduced even further in an effort to be able to see the quantum dot emission (Figure 4.1). In the emission spectra of decreasing protein to quantum dot ratios, the tail end of the spectra is observed to becoming longer with a increasing ratio of quantum dots. The presence of increased quantum dots in relation to protein demonstrates an observable effect in the bioluminescence of the protein.

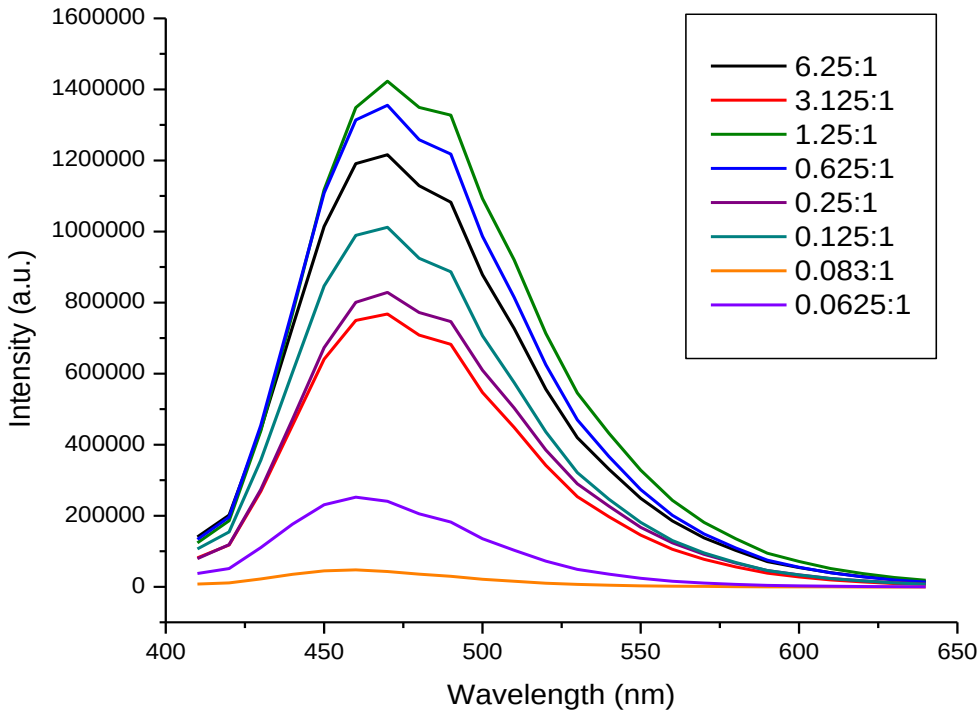

Figure 4.2: Bioluminescence using various ratios of protein to quantum dots from 6.25:1 to 0.0625:1.

The ratio between the protein to quantum dot was adjusted even further in an effort to be able to observe a second peak of intensity emitted by the quantum dots. Results indicate the peak is not observable despite drastically reducing the bioluminescence emission (Figure 4.2). Despite no discernable peak observable in the wavelength pertaining to the quantum dots, the bioluminescence of the protein was decreased considerably. Further experiments used a ratio of 0.0625:1 to ensure a sufficient amount of bioluminescence but also in the hopes of being able to observe the quantum dot peaks by adjusting other properties of the sensor.

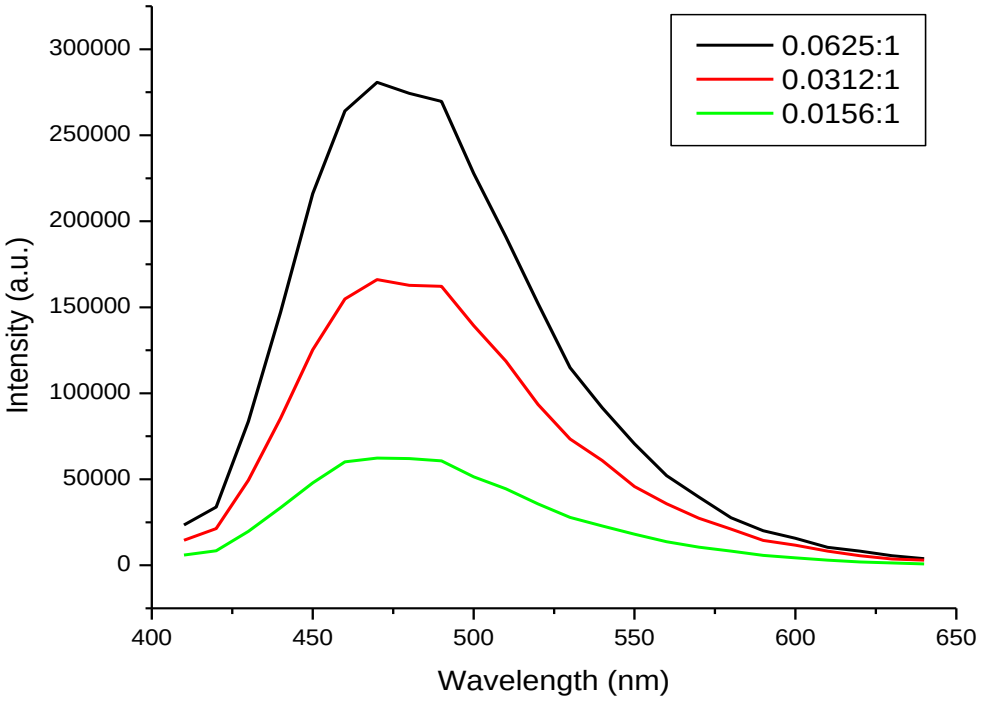

Figure 4.3: Bioluminescence using various ratios of protein to quantum dots from 0.0625:1 to 0.0156:1

4.3 EDC to quantum dot ratio

EDC to quantum dot ratio is important to maintain at a ratio, which allows for the most efficient conjugation between the QDs and protein to occur. However, it is important to note that too high of a ratio of EDC to QD may result in aggregation and precipitation of the sensor components [44]. The results indicate that the ratios of EDC to QD from 10000:1, 500:1, and 250:1 result in a similar bioluminescence emission. However, using a ratio of 100:1 resulted in significantly increased bioluminescence emission when compared to other ratios (Figure 4.3).

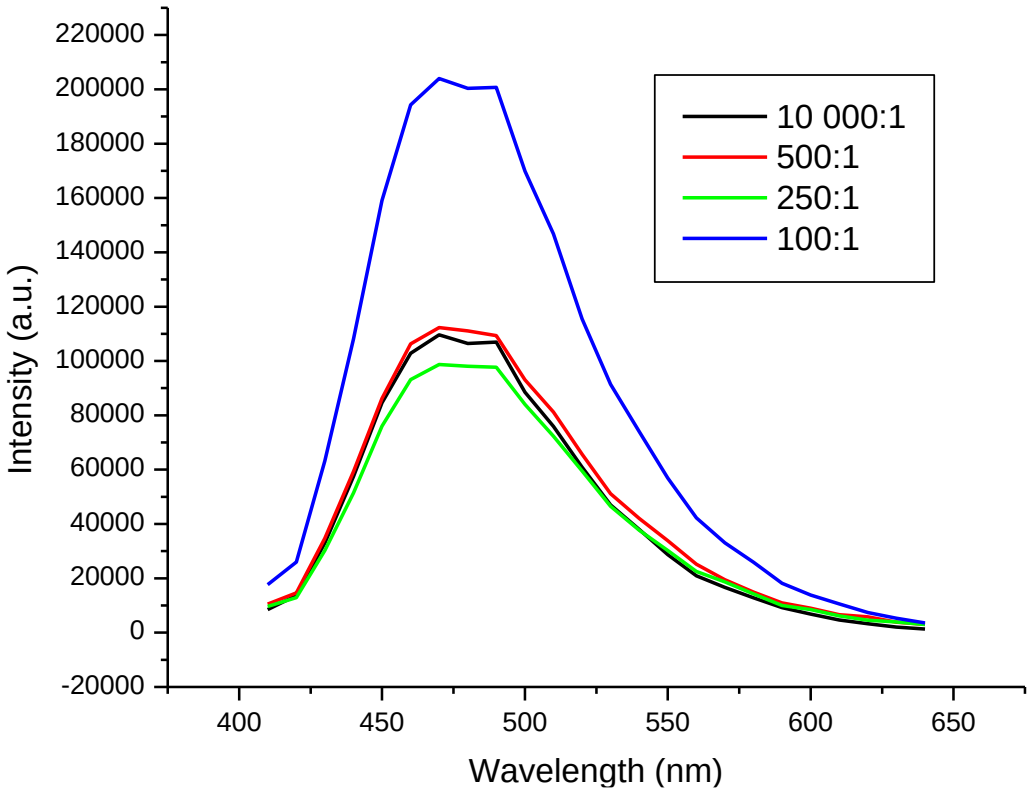

Figure 4.4: Bioluminescence for homogenous sensor samples conjugated using varying ratios of EDC to quantum dots. Ratios range from 10 000:1 to 100:1

4.4 Conjugation time

Conjugation time is important to control due to the balance between the QD and protein conjugation and the protein conjugating with other protein. Having an increased conjugation time resulted in a significantly higher protein emission and a lower QD emission. The ideal conjugation time would allow enough of the QD and protein to conjugate, while keeping the amount of protein conjugating to each other at the minimum.

The conjugation of the homogenous sensor was tested at times of 30 minutes, 1 hour, 2 hours, 4 hours, and 6 hours. As the time of conjugation increases, the bioluminescence emission intensity also decreases (Figure 4.4). The increase in conjugation time leads to a increase in interactions between proteins which lead to aggregation and decreased bioluminescence.

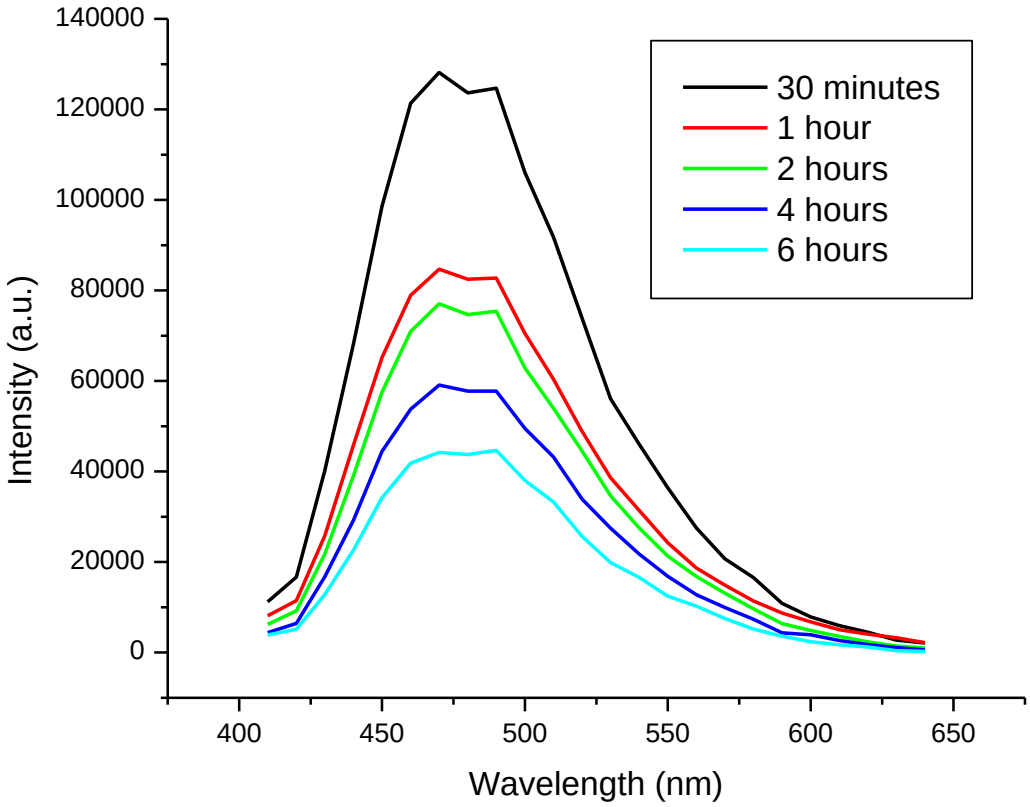

Figure 4.5: Bioluminescence for homogenous sensor samples conjugated for varying lengths of time. Time ranges from 30 minutes to 6 hours.

4.5 Evaluation of the homogenous BRET sensor with increasing glucose concentration

In order for the sensor to be applicable in physiological conditions, the sensor should demonstrate a quantifiable difference when there are varying concentrations of glucose present in the medium. The performance of the sensor under varying concentration of glucose was evaluated using a 5:16 protein to quantum dot ratio, 100:1 EDC to quantum dot ratio and 1 hour of incubation time. Increasing the glucose concentration resulted in a significantly lower emission of the luciferase.

Results indicate a significant decrease in bioluminescence intensity for increases in glucose concentration (Figure 4.5). This is due to increases in BRET events as glucose concentration increases. An increase in glucose concentration results in bioluminescence

being absorbed by the quantum dots, thereby decreasing the measured bioluminescence intensity.

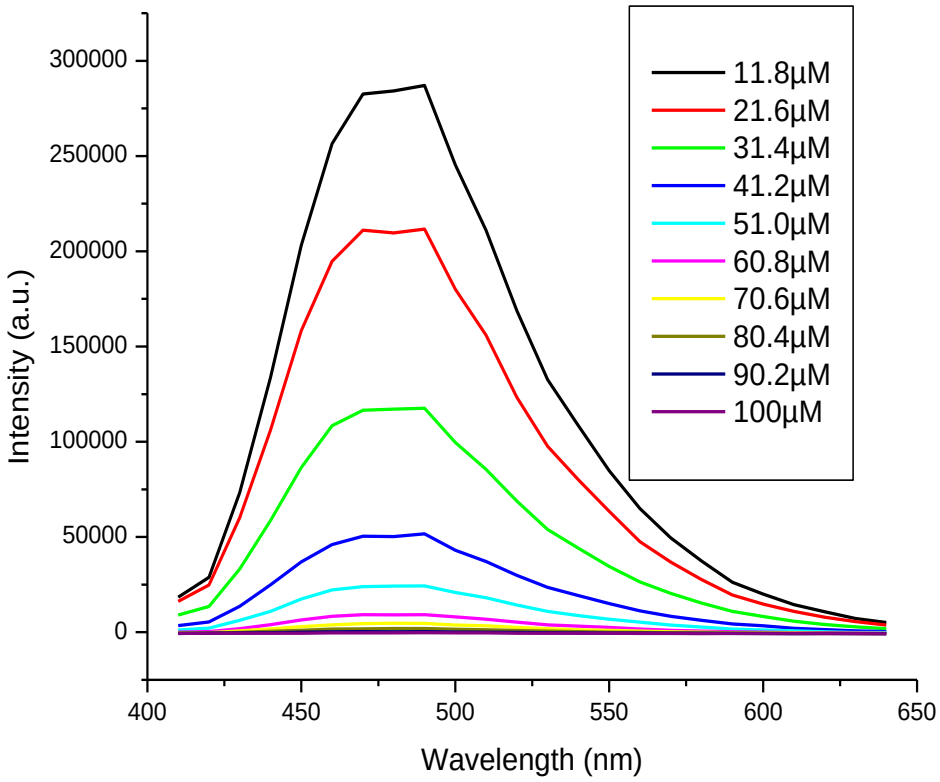

Figure 4.6: Bioluminescence intensity using increasing concentrations of glucose.

4.6 Evaluation of the decay in bioluminescence in the homogenous BRET sensor with a fixed glucose concentration

The decay of the bioluminescence by the protein was evaluated using different concentrations of glucose over a fixed period of time after adding the CTZ. The initial spectrum was measured immediately after the addition of CTZ and following spectra was measured immediately following the conclusion of the measurement of the spectrum before it. The total time for measuring each spectrum was 10 seconds. Testing was done to evaluate how rapidly the bioluminescence of the protein will decay for a set period of time and whether the emission spectra of the sensor would show a discernable peak for the

quantum dots. Results indicate significantly larger decay in bioluminescence during earlier time intervals for all concentrations of glucose used (Figure 4.6). Considering the large decay observed within a short period of time after adding the CTZ, all future testing should seek to measure the fluorescence as soon as possible in order to obtain strong bioluminescence.

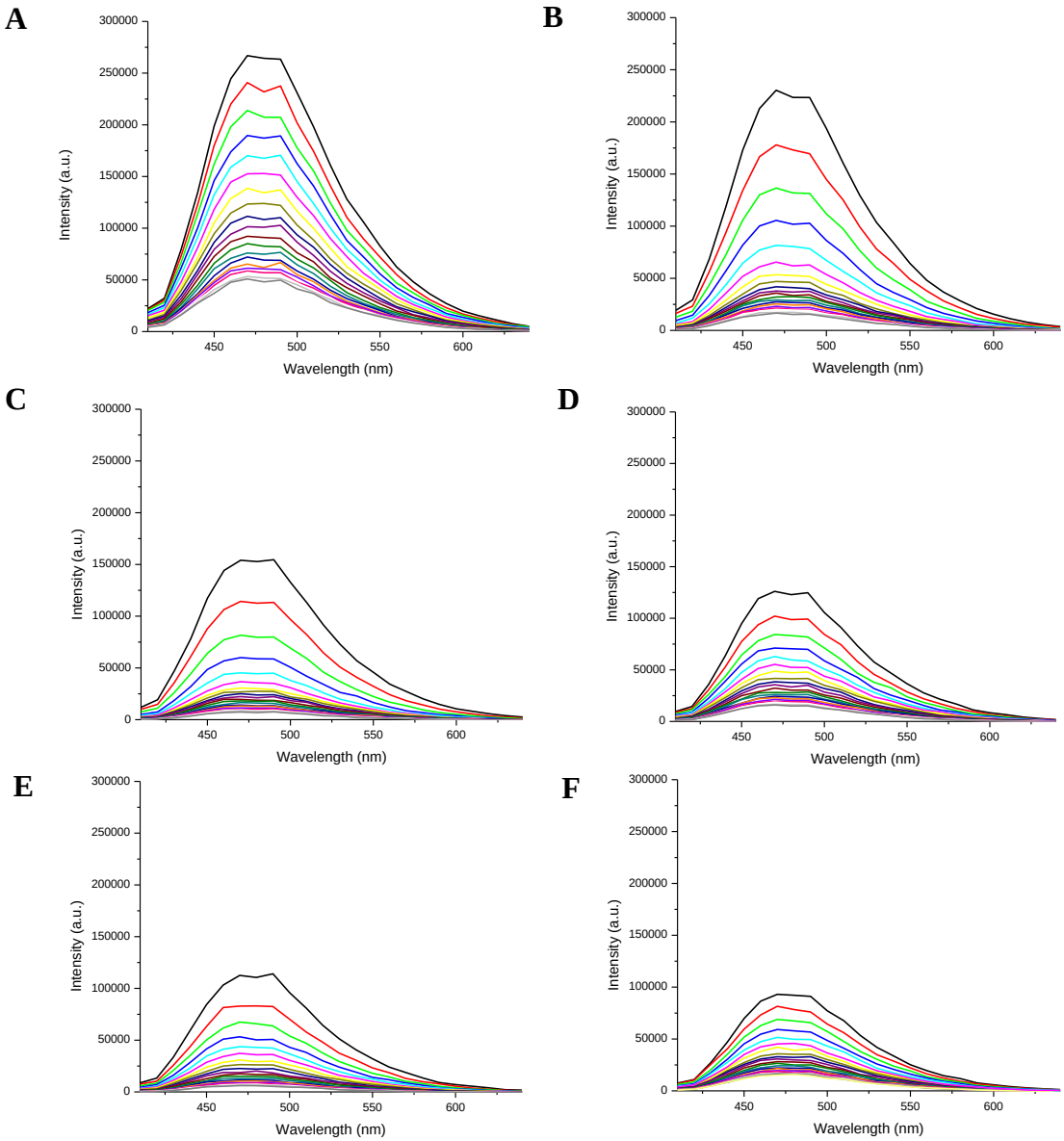

Figure 4.7: Decay of bioluminescence in 10s intervals for a protein to quantum ratio of 0.0312:1 in glucose concentrations of (A) 2 µM, (B) 100 µM, (C) 1550 µM, (D) 3000 µM, (E) 6500 µM, and (F) 10 000 µM.

The effect of filtering the sensor solution was evaluated, in addition to the effect of adding glucose to the filtered solution. Results indicate a significant decrease when the sensor solution is unfiltered or filtered through a centrifugal filter. For the solution containing a ratio of 0.0312:1 and 0.0156:1, there exists a significant difference when glucose is added to the filtered solution compared to the other two conditions (Figure 4.7). Without filtering the sensor solution, free GBP and potentially free QDs remain which results in an increased bioluminescence emission. Filtering the solution for future studies could prove to be effective in removing any bioluminescence that does not come from the conjugated BRET sensor.

A

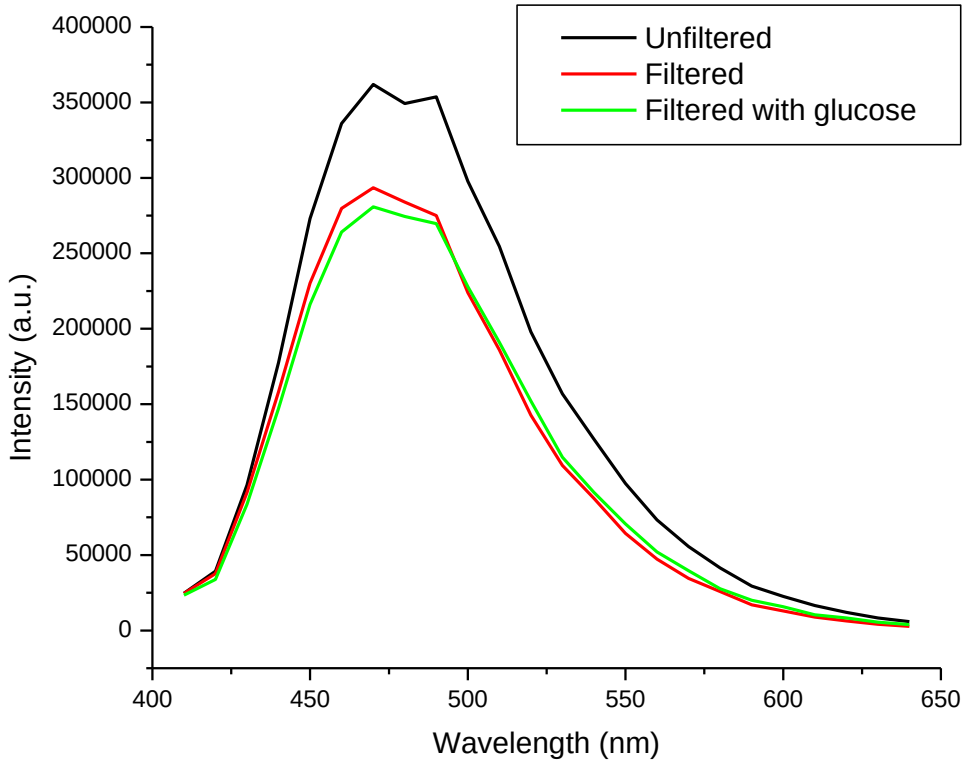

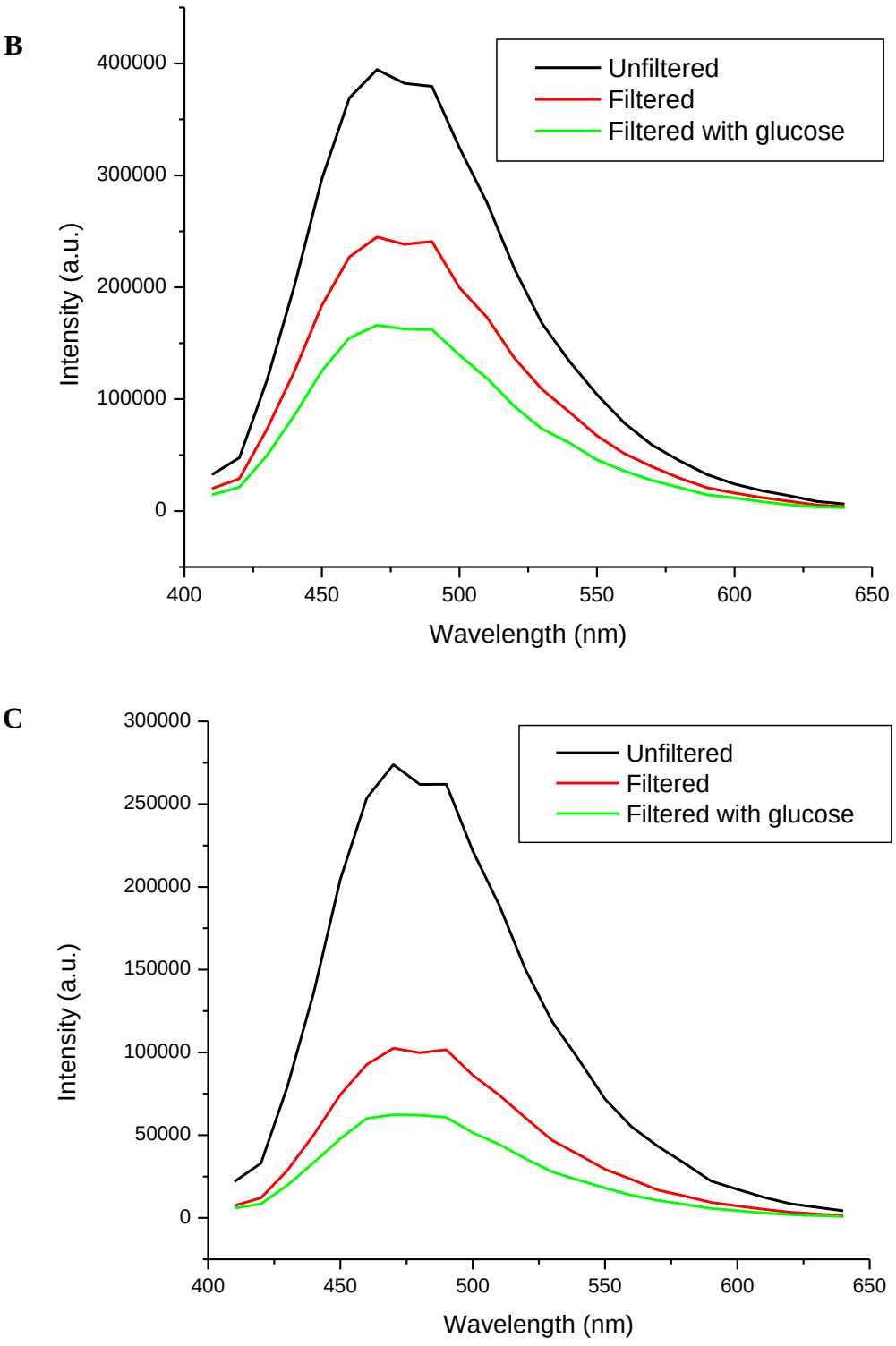

Figure 4.8: Bioluminescence of sensor when unfiltered, filtered, and with glucose added for ratios of (A) 0.0625:1, (B) 0.0312:1, and (C) 0.0156:1.

The lack of a discernable peak for the QDs is not an indication that BRET did not occur. It may be possible that the band gap of the QDs may be too large and requires too much energy to become excited. In the future, QDs with smaller band gaps could be chosen to increase the possibility of BRET occurring in the sensor. The intensity required from the bioluminescence in proportion to the QD emission may be so large that the QD emission is undetectable when compared to the tail end of the bioluminescence peak.

4.7 Conjugation of sensor onto a solid substrate

TEM imaging of CdTe QDs decorated with ZnO nanoarray (ZnO-CdTe QD) was used to determine the diameter of the ZnO nanoarray (Figure 5.2). It was estimated to be 230 ± 10nm and the average particle size of CdTe QDs is around 10 ± 3nm (Appendix, Figure 1).

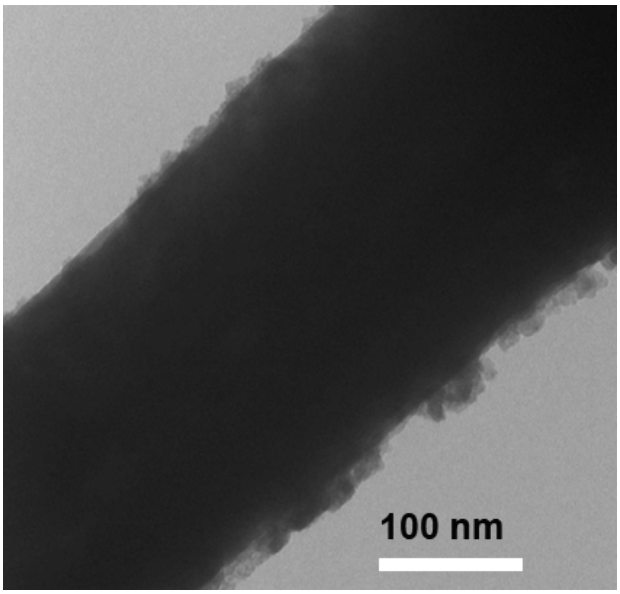

Figure 4.9: TEM micrograph of CdTe decorated with ZnO nanoarray (courtesy of Dr. Yi Chen).

SEM micrograph of the solid sample was used to determine the length of each nanorod. Each nanorod was estimated to be 3.0 ± 0.2μm (Figure 5.3A). The photoluminescence of the CdTe QDs and ZnO-CdTe QD was measured using an excitation wavelength of 480nm. The maximum emission of CdTe QDs modified with thioglycolic acid (TGA) is

centered at 617nm, while the emission of ZnO-CdTe QDs had a red shift to 620nm (Figure 5.3B).

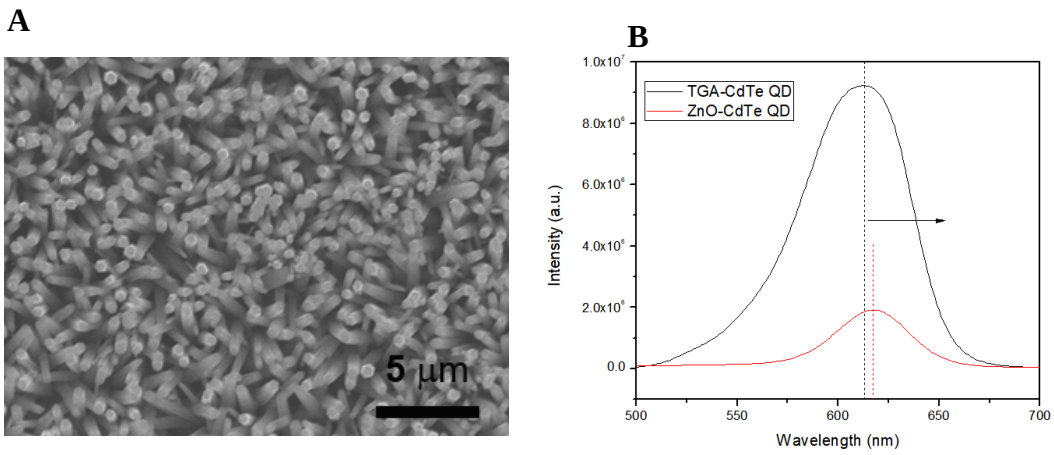

Figure 4.10: (A) SEM micrograph of CdTe decorated ZnO nanorod (courtesy of Yi Chen); (B) Photoluminescence of CdTe QDs and CdTe decorated ZnO nanorods (courtesy of Yi Chen)

Addition of 2µM of 10mM glucose then 5µM of 1mM CTZ to the solid substrate resulted in an observable increase in photoluminescence intensity peak around 480nm. The emission peak corresponds to the peak emission of Rluc; therefore, the protein was successfully conjugated to the solid substrate. The quantum dot emission was not verifiable; however, it may have been too low to detect (Figure 5.4).

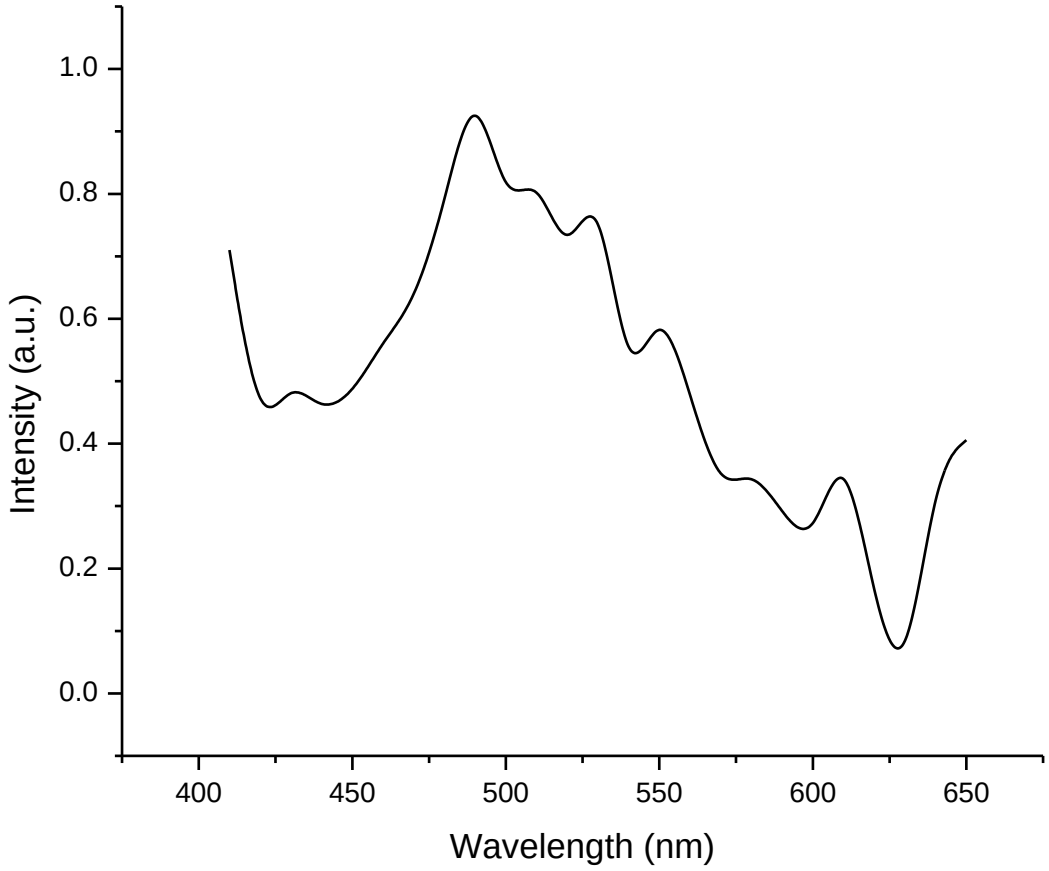

Figure 4.11: Normalized fluorescence emission of ZnO nanorod array on PDMS film conjugated with quantum dots (CdTe) and recombinant protein (GBP-Rluc) using EDC.

4.8 Refinement of conjugation process

Conjugation of the sensor onto the ZnO nanorod array may require different ideal conditions such as conjugation time, EDC to QD ratio, and such. Therefore, more testing is required to fully optimize the sensor on a solid substrate. The concentration of EDC to be used during the conjugation of both the CdTe and the recombinant protein should be adjusted to find the ideal ratio. The concentration of the CdTe per area of the solid substrate should also be adjusted accordingly.

Chapter 5

5 Discussion

The results show an ideal ratio of components to be used during the conjugation process. When comparing ratios of an increasing concentration of quantum dots compared to the recombinant protein, the bioluminescence decreased significantly. As the ratio of quantum dots increases, there is a larger ratio of acceptor molecules compared to donor molecules. Therefore, more of the bioluminescence emitted by the recombinant protein is absorbed by the quantum dots, which leads to a decrease seen in the bioluminescence intensity found at 480nm. From these results, it is concluded that BRET is occurring between the recombinant protein and the quantum dots, and allows us to select a ratio of protein to quantum dots to be used in further experiments. The fluorescence readings did not show a discernable peak from the quantum dots, however, it was concluded that the intensity of the bioluminescence from the recombinant protein was masking the quantum dot emission. Despite adjusting the ratio of the donor and acceptor, the quantum dot emission could not be observed, therefore the ratio selected for further experiments was 0.0625:1. Using a ratio of 0.0625:1 ensured a sufficient amount of bioluminescence but also was chosen in the hopes of observing the quantum dot emission when adjusting other factors.

The ratio of EDC to quantum dots for the purposes of bioconjugation was adjusted to find the ideal concentration of EDC to use. Using an excess amount of EDC may result in aggregation and precipitation of the sensor components [142], therefore the ratio was adjusted to avoid such an event. The ratio of 100:1 EDC to quantum dots was found to have the highest intensity of bioluminescence, which was concluded to be the result of the most efficient conjugation without the loss of bioluminescence due to protein aggregation or precipitation.

Conjugation time was varied to determine the ideal reaction time to achieve the most efficient bioconjugation. The conjugation time is important to control, otherwise allowing component to react for too long may lead to aggregation and precipitation of sensor components [142]. A conjugation time of 30 minutes yielded the highest

bioluminescence, thereby indicating the most efficient conjugation with the least amount of sensor component precipitation.

The integral finding was the results about the change in bioluminescence as glucose concentration is increased. Increasing glucose concentration resulted in a decrease bioluminescence. This indicates a BRET reaction which is evident by the decrease in bioluminescence which can be attributed to absorption of the bioluminescence light energy by the quantum dots. An increase in glucose concentration allows for more of the glucose binding protein to change conformation and allow the BRET pair come into close enough distance to initiate an energy transfer. Sensors to detect glucose, which have been developed in the past, have utilized fluorescent proteins as acceptors or fluorescent protein as donors instead of bioluminescent protein. In the present, there does not exist a sensor for detecting glucose that combines the biocompatibility of light emitting enzymes from animals and functionalized quantum dots.

The sensor, when conjugated to the ZnO nanorod array, exhibited characteristic peaks of emission at 480nm and 565nm. These peaks indicate the successful conjugation of the sensor onto the substrate, as well as the incidence of a BRET event. Zinc oxide has a known emission peak at about 380nm [143], which can be observed in the photoluminescence spectra, however the spectra does not completely capture the peak.

Chapter 6

6 Summary and future works

As the number of diabetes patients increases worldwide, the demand for a non-invasive and accurate method for detecting glucose increases. The measurement of different body fluids has been explored. Tear glucose in particular shows promise due to its strong correlation with blood glucose based on previous research. Due to the low concentrations of glucose in tears, FRET and by extension, BRET has been employed to measure these concentrations in part due to the extremely sensitive nature of the techniques. Due to the external energy requirement of FRET, BRET is the ideal choice due to its biocompatibility and lack of drawbacks presented by requiring an external energy source. The combination

of BRET and a glucose binding protein has not been extensively reported on. Therefore, we have a developed a BRET sensor incorporating glucose binding protein and quantum dots in order to measure low concentrations of glucose. Upon binding of the glucose binding protein, it will change conformation, bringing a bioluminescent protein and the quantum dots close enough to trigger BRET. Quantum dots were chosen due to having unique optical properties and proven effectiveness in BRET constructs. They are an excellent alternative to organic dyes and further evidence continues to build up in favor of their advantages.

Trends regarding the bioluminescence were observed in the results. Firstly, decreasing the ratio of protein to quantum dot resulted in decreased bioluminescence. Secondly, an increased concentration of quantum dots has an observable, negative effect on the intensity of the bioluminescence. Thirdly, for varying concentrations of EDC, only low ratios of EDC to quantum dots had any observable effect on the intensity of the bioluminescence. A ratio of 100:1 EDC to quantum dots significantly increased the bioluminescence intensity when compared to other ratios. In addition, conjugation time had a significant impact on the bioluminescence intensity. Increasing conjugation times resulted in significantly lower bioluminescence intensity. Further, for increasing concentrations of glucose added in to the homogenous sensor, bioluminescence intensity decreased. Moreover, tests performed to measure the decay of the bioluminescence intensity over time demonstrated that intensity decreased significantly faster at earlier time points than later time points. Therefore, tests regarding bioluminescence intensity should be performed and measured immediately after the addition of CTZ. Finally, filtering the sensor after the conjugation procedure had a significant effect on the bioluminescence intensity.

Trends observed in bioluminescence indicate that the construct is particularly sensitive to small changes in components used to synthesize the sensor. However, once the ideal ratios of each component are found, the sensor will provide consistent results to increase its applicability in the task of measuring blood glucose levels.

Experiments regarding the deposition of the sensor onto a ZnO nanorod array were able to demonstrate successful deposition. Bioluminescence was observed when CTZ was added

to the substrate, therefore it can be concluded that the protein had successfully conjugated to the functionalized quantum dots on the surface of the ZnO nanorod array. Further testing will be required to optimize the conjugation of the BRET pair and increase the bioluminescence.

The development of a BRET sensor utilizing nanomaterials to detect glucose is a novel design and has not been investigated before. This sensor construct promises to be a simple and non-invasive method through implementation with a transducer to monitor glucose concentrations in tears to output an accurate reading of blood glucose. This construct utilizes quantum dots synthesized in a simple and facile process and combines them with biocompatible proteins to detect glucose concentrations as low as

The results indicate difficulty in identifying a BRET signal as a result of energy transfer between the protein and the quantum dots. Further findings led to the conclusion that BRET is occurring, however the emission from the quantum dots is too low to detect when compared to the high intensity of the Rluc bioluminescence. Futures studies should focus on utilizing quantum dots with a smaller band gap, thereby requiring less energy from the bioluminescence to excite. Therefore, increased quantum dot emission could potentially be observed.

In the future, different luciferases could be implemented in place of *Renilla* luciferase such as Nano luciferase, a smaller variant which has been proven to be robust and highly sensitive. Its size has proven to a valuable asset in the bioconjugation process. In addition, due to the non-specific nature of the bioconjugation process, other binding proteins could potentially replace the glucose binding protein. This could lead to applications of the sensor for detecting other small molecules besides glucose. Finally, optimizations in order to improve the performance of the sensor in a solid substrate can be implemented. Such optimizations may include the amount of EDC to be used for conjugated both the CdTe and the recombinant protein, and the specific concentration of CdTe to be used per area of the solid substrate.

References

1. Collaboration, E. R. F.; Sarwar, N.; Gao, P.; Seshasai, S. R. K.; Gobin, R.; Kaptoge, S.; Di Angelantonio, E.; Ingelsson, E.; Lawlor, D. A.; Selvin, E.; et al. Diabetes mellitus, fasting blood glucose concentration, and risk of vascular disease: a collaborative meta-analysis of 102 prospective studies. *Lancet (London, England)* **2010**, *375*, 2215–2222.

2. FDA Blood Glucose Monitoring Devices <https://www.fda.gov/medical-devices/vitro-diagnostics/blood-glucose-monitoring-devices> (accessed Jul 25, 2019).

3. Hannon, T. S.; Yazel-Smith, L. G.; Hatton, A. S.; Stanton, J. L.; Moser, E. A. S.; Li, X.; Carroll, A. E. Advancing diabetes management in adolescents: Comparative effectiveness of mobile self-monitoring blood glucose technology and family-centered goal setting. *Pediatr. Diabetes* **2018**, *19*, 776–781.

4. Vishnu, N.; Sahatiya, P.; Kong, C. Y.; Badhulika, S. Large area, one step synthesis of NiSe2 films on cellulose paper for glucose monitoring in bio-mimicking samples for clinical diagnostics. *Nanotechnology* **2019**, *30*, 355502.

5. Mohammadifar, M.; Tahernia, M.; Choi, S. An Equipment-Free, Paper-Based Electrochemical Sensor for Visual Monitoring of Glucose Levels in Urine. *SLAS Technol.* **2019**, 2472630319846876.

6. Zhao, Y.; Zhai, Q.; Dong, D.; An, T.; Gong, S.; Shi, Q.; Cheng, W. Highly Stretchable and Strain-Insensitive Fiber-Based Wearable Electrochemical Biosensor to Monitor Glucose in the Sweat. *Anal. Chem.* **2019**, *91*, 6569–6576.

7. Salim, A.; Lim, S. Recent advances in noninvasive flexible and wearable wireless biosensors. *Biosens. Bioelectron.* **2019**, *141*, 111422.

8. Zhao, J.; Lin, Y.; Wu, J.; Nyein, H. Y. Y.; Bariya, M.; Tai, L.-C.; Chao, M.; Ji, W.; Zhang, G.; Fan, Z.; et al. A Fully Integrated and Self-Powered Smartwatch for Continuous Sweat Glucose Monitoring. *ACS sensors* **2019**.

9. Sempionatto, J. R.; Brazaca, L. C.; Garcia-Carmona, L.; Bolat, G.; Campbell, A. S.;

Martin, A.; Tang, G.; Shah, R.; Mishra, R. K.; Kim, J.; et al. Eyeglasses-based tear biosensing system: Non-invasive detection of alcohol, vitamins and glucose. *Biosens. Bioelectron.* **2019**, *137*, 161–170.

10. Lin, Y.-R.; Hung, C.-C.; Chiu, H.-Y.; Chang, B.-H.; Li, B.-R.; Cheng, S.-J.; Yang, J.-W.; Lin, S.-F.; Chen, G.-Y. Noninvasive Glucose Monitoring with a Contact Lens and Smartphone. *Sensors (Basel).* **2018**, *18*.

11. Price, C. P. Point-of-care testing in diabetes mellitus. *Clin. Chem. Lab. Med.* **2003**, *41*, 1213–1219.

12. Weibel, M. K.; Bright, H. J. The glucose oxidase mechanism. Interpretation of the pH dependence. *J. Biol. Chem.* **1971**, *246*, 2734–2744.

13. Guilbault, G. G.; Lubrano, G. J. An enzyme electrode for the amperometric determination of glucose. *Anal. Chim. Acta* **1973**, *64*, 439–455.

14. Turner, A. P.; Chen, B.; Piletsky, S. A. In vitro diagnostics in diabetes: meeting the challenge. *Clin. Chem.* **1999**, *45*, 1596–1601.

15. Nie, S.; Emory, S. R. Probing Single Molecules and Single Nanoparticles by Surface-Enhanced Raman Scattering. *Science (80-.).* **1997**, *275*, 1102 LP – 1106.

16. Förster, T. Zwischenmolekulare Energiewanderung und Fluoreszenz. *Ann. Phys.* **1948**, *437*, 55–75.

17. Morin, J. G.; Hastings, J. W. Energy transfer in a bioluminescent system. *J. Cell. Physiol.* **1971**, *77*, 313–318.

18. Ward, W. W.; Cormier, M. J. An energy transfer protein in coelenterate bioluminescence. Characterization of the Renilla green-fluorescent protein. *J. Biol. Chem.* **1979**, *254*, 781–788.

19. Lorenz, W. W.; McCann, R. O.; Longiaru, M.; Cormier, M. J. Isolation and expression of a cDNA encoding Renilla reniformis luciferase. *Proc. Natl. Acad. Sci.*

1991, *88*, 4438 LP – 4442.

20. Pfleger, K. D. G.; Eidne, K. A. Illuminating insights into protein-protein interactions using bioluminescence resonance energy transfer (BRET). *Nat. Methods* **2006**, *3*, 165–174.

21. del Rosal, B.; Benayas, A. Strategies to Overcome Autofluorescence in Nanoprobe-Driven In Vivo Fluorescence Imaging. *Small Methods* **2018**, *2*, 1800075.

22. So, M.-K.; Xu, C.; Loening, A. M.; Gambhir, S. S.; Rao, J. Self-illuminating quantum dot conjugates for in vivo imaging. *Nat. Biotechnol.* **2006**, *24*, 339.

23. Troy, T.; Jekic-McMullen, D.; Sambucetti, L.; Rice, B. Quantitative Comparison of the Sensitivity of Detection of Fluorescent and Bioluminescent Reporters in Animal Models. *Mol. Imaging* **2004**, *3*, 9–23.

24. Zhao, S.; Huang, Y.; Shi, M.; Liu, R.; Liu, Y.-M. Chemiluminescence resonance energy transfer-based detection for microchip electrophoresis. *Anal. Chem.* **2010**, *82*, 2036–2041.

25. Huang, X.; Li, L.; Qian, H.; Dong, C.; Ren, J. A resonance energy transfer between chemiluminescent donors and luminescent quantum-dots as acceptors (CRET). *Angew. Chem. Int. Ed. Engl.* **2006**, *45*, 5140–5143.

26. Chan, W. C.; Nie, S. Quantum dot bioconjugates for ultrasensitive nonisotopic detection. *Science* **1998**, *281*, 2016–2018.

27. Bruchez, M. J.; Moronne, M.; Gin, P.; Weiss, S.; Alivisatos, A. P. Semiconductor nanocrystals as fluorescent biological labels. *Science* **1998**, *281*, 2013–2016.

28. Ward, W. W.; Cormier, M. J. ENERGY TRANSFER VIA PROTEIN-PROTEIN INTERACTION IN RENILLA BIOLUMINESCENCE. *Photochem. Photobiol.* **1978**, *27*, 389–396.

29. Schaufele, F.; Demarco, I.; Day, R. N. FRET Imaging in the Wide-Field Microscope.

In *Molecular Imaging*; PERIASAMY, A.; DAY, R. N. B. T.-M. I., Eds.; American Physiological Society: San Diego, 2005; pp. 72–94.

30. Ansbacher, T.; Srivastava, H. K.; Stein, T.; Baer, R.; Merkx, M.; Shurki, A. Calculation of transition dipole moment in fluorescent proteins—towards efficient energy transfer. *Phys. Chem. Chem. Phys.* **2012**, *14*, 4109–4117.

31. Hsu, C.-Y.; Chen, C.-W.; Yu, H.-P.; Lin, Y.-F.; Lai, P.-S. Bioluminescence resonance energy transfer using luciferase-immobilized quantum dots for self-illuminated photodynamic therapy. *Biomaterials* **2013**, *34*, 1204–1212.

32. Mukhopadhyay, P.; Maity, S.; Mandal, S.; Chakraborti, A. S.; Prajapati, A. K.; Kundu, P. P. Preparation, characterization and in vivo evaluation of pH sensitive, safe quercetin-succinylated chitosan-alginate core-shell-corona nanoparticle for diabetes treatment. *Carbohydr. Polym.* **2018**, *182*, 42–51.

33. Gao, X.; Chan, W. C. W.; Nie, S. Quantum-dot nanocrystals for ultrasensitive biological labeling and multicolor optical encoding. *J. Biomed. Opt.* **2002**, *7*, 532–537.

34. Michalet, X.; Pinaud, F. F.; Bentolila, L. A.; Tsay, J. M.; Doose, S.; Li, J. J.; Sundaresan, G.; Wu, A. M.; Gambhir, S. S.; Weiss, S. Quantum dots for live cells, in vivo imaging, and diagnostics. *Science* **2005**, *307*, 538–544.

35. Smith, A. M.; Gao, X.; Nie, S. Quantum dot nanocrystals for in vivo molecular and cellular imaging. *Photochem. Photobiol.* **2004**, *80*, 377–385.

36. Hoshino, H.; Nakajima, Y.; Ohmiya, Y. Luciferase-YFP fusion tag with enhanced emission for single-cell luminescence imaging. *Nat. Methods* **2007**, *4*, 637.

37. Iglesias, P.; Costoya, J. A. A novel BRET-based genetically encoded biosensor for functional imaging of hypoxia. *Biosens. Bioelectron.* **2009**, *24*, 3126–3130.

38. Rumyantsev, K. A.; Turoverov, K. K.; Verkhusha, V. V Near-infrared bioluminescent proteins for two-color multimodal imaging. *Sci. Rep.* **2016**, *6*, 36588.

39. Kojima, R.; Takakura, H.; Ozawa, T.; Tada, Y.; Nagano, T.; Urano, Y. Rational Design and Development of Near-Infrared-Emitting Firefly Luciferins Available In Vivo. *Angew. Chemie Int. Ed.* **2012**, *52*, 1175–1179.

40. Wu, C.; Mino, K.; Akimoto, H.; Kawabata, M.; Nakamura, K.; Ozaki, M.; Ohmiya, Y. In vivo far-red luminescence imaging of a biomarker based on BRET from Cypridina bioluminescence to an organic dye. *Proc. Natl. Acad. Sci.* **2009**, *106*, 15599 LP – 15603.

41. De, A. The New Era of Bioluminescence Resonance Energy Transfer Technology. *Curr. Pharm. Biotechnol.* 2011, *12*, 558–568.

42. Xia, Z.; Rao, J. Biosensing and imaging based on bioluminescence resonance energy transfer. *Curr. Opin. Biotechnol.* **2009**, *20*, 37–44.

43. Iga, A. M.; Robertson, J. H. P.; Winslet, M. C.; Seifalian, A. M. Clinical potential of quantum dots. *J. Biomed. Biotechnol.* **2007**, *2007*, 76087.

44. Medintz, I. L.; Uyeda, H. T.; Goldman, E. R.; Mattoussi, H. Quantum dot bioconjugates for imaging, labelling and sensing. *Nat. Mater.* **2005**, *4*, 435–446.

45. Gerion, D.; Pinaud, F.; Williams, S. C.; Parak, W. J.; Zanchet, D.; Weiss, S.; Alivisatos, A. P. Synthesis and Properties of Biocompatible Water-Soluble Silica-Coated CdSe/ZnS Semiconductor Quantum Dots. *J. Phys. Chem. B* **2001**, *105*, 8861–8871.

46. Mattoussi, H.; Mauro, J. M.; Goldman, E. R.; Anderson, G. P.; Sundar, V. C.; Mikulec, F. V; Bawendi, M. G. Self-Assembly of CdSe−ZnS Quantum Dot Bioconjugates Using an Engineered Recombinant Protein. *J. Am. Chem. Soc.* **2000**, *122*, 12142–12150.

47. Zhang, J.-Y.; Wang, X.-Y.; Xiao, M.; Ye, Y.-H. Modified spontaneous emission of CdTe quantum dots inside a photonic crystal. *Opt. Lett.* **2003**, *28*, 1430–1432.

48. Gaponik, N.; Talapin, D. V; Rogach, A. L.; Hoppe, K.; Shevchenko, E. V; Kornowski, A.; Eychmüller, A.; Weller, H. Thiol-Capping of CdTe Nanocrystals: An

Alternative to Organometallic Synthetic Routes. *J. Phys. Chem. B* **2002**, *106*, 7177–7185.

49. Zhang, H.; Wang, L. P.; Xiong, H. M.; Hu, L. H.; Yang, B.; Li, W. Hydrothermal Synthesis for High-Quality CDTe Nanocrystals. *Adv. Mater.* **2003**, *15*, 1712–1715.

50. De, A. The New Era of Bioluminescence Resonance Energy Transfer Technology. *Curr. Pharm. Biotechnol.* 2011, *12*, 558–568.

51. Alam, R.; Karam, L. M.; Doane, T. L.; Zylstra, J.; Fontaine, D. M.; Branchini, B. R.; Maye, M. M. Near infrared bioluminescence resonance energy transfer from firefly luciferase—quantum dot bionanoconjugates. *Nanotechnology* **2014**, *25*, 495606.

52. Mithöfer, A.; Mazars, C. Aequorin-based measurements of intracellular Ca2+-signatures in plant cells. *Biol. Proced. Online* **2002**, *4*, 105–118.

53. Lim, D.; Bertoli, A.; Sorgato, M. C.; Moccia, F. Generation and usage of aequorin lentiviral vectors for Ca2+ measurement in sub-cellular compartments of hard-to-transfect cells. *Cell Calcium* **2016**, *59*, 228–239.

54. Cobbold, P. H.; Cuthbertson, K. S.; Goyns, M. H.; Rice, V. Aequorin measurements of free calcium in single mammalian cells. *J. Cell Sci.* **1983**, *61*, 123–136.

55. Granatiero, V.; Patron, M.; Tosatto, A.; Merli, G.; Rizzuto, R. The use of aequorin and its variants for Ca2+ measurements. *Cold Spring Harb. Protoc.* **2014**, *2014*, 9–16.

56. Zeinoddini, M.; Khajeh, K.; Hosseinkhani, S.; Saeedinia, A. R.; Robatjazi, S.-M. Stabilisation of Recombinant Aequorin by Polyols: Activity, Thermostability and Limited Proteolysis. *Appl. Biochem. Biotechnol.* **2013**, *170*, 273–280.

57. Iwano, S.; Sugiyama, M.; Hama, H.; Watakabe, A.; Hasegawa, N.; Kuchimaru, T.; Tanaka, K. Z.; Takahashi, M.; Ishida, Y.; Hata, J.; et al. Single-cell bioluminescence imaging of deep tissue in freely moving animals. *Science (80-.).* **2018**, *359*, 935–939.

58. Waidmann, M. S.; Bleichrodt, F. S.; Laslo, T.; Riedel, C. U. Bacterial luciferase reporters: the Swiss army knife of molecular biology. *Bioeng. Bugs* **2011**, *2*, 8–16.

59. Ke, D.; Tu, S.-C. Activities, Kinetics and Emission Spectra of Bacterial Luciferase-Fluorescent Protein Fusion Enzymes. *Photochem. Photobiol.* **2011**, *87*, 1346–1353.

60. Cui, B.; Zhang, L.; Song, Y.; Wei, J.; Li, C.; Wang, T.; Wang, Y.; Zhao, T.; Shen, X. Engineering an Enhanced, Thermostable, Monomeric Bacterial Luciferase Gene As a Reporter in Plant Protoplasts. *PLoS One* **2014**, *9*.

61. Hollis, R. P.; Lagido, C.; Pettitt, J.; Porter, A. J. R.; Killham, K.; Paton, G. I.; Glover, L. A. Toxicity of the bacterial luciferase substrate, n-decyl aldehyde, to Saccharomyces cerevisiae and Caenorhabditis elegans. *FEBS Lett.* **2001**, *506*, 140–142.

62. Coleman, S. M.; McGregor, A. A bright future for bioluminescent imaging in viral research. *Future Virol.* **2015**, *10*, 169–183.

63. de Wet, J. R.; Wood, K. V; DeLuca, M.; Helinski, D. R.; Subramani, S. Firefly luciferase gene: structure and expression in mammalian cells. *Mol. Cell. Biol.* **1987**, *7*, 725–737.

64. Lundin, A. Optimization of the Firefly Luciferase Reaction for Analytical Purposes. In *Bioluminescence: Fundamentals and Applications in Biotechnology - Volume 2*; Thouand, G.; Marks, R., Eds.; Advances in Biochemical Engineering/Biotechnology; Springer Berlin Heidelberg: Berlin, Heidelberg, 2014; pp. 31–62.

65. Gibbons, A. E.; Luker, K. E.; Luker, G. D. Dual Reporter Bioluminescence Imaging with NanoLuc and Firefly Luciferase BT - Reporter Gene Imaging: Methods and Protocols. In; Dubey, P., Ed.; Springer New York: New York, NY, 2018; pp. 41–50.

66. Branchini, B. R.; Southworth, T. L.; Fontaine, D. M.; Kohrt, D.; Welcome, F. S.; Florentine, C. M.; Henricks, E. R.; DeBartolo, D. B.; Michelini, E.; Cevenini, L.; et al. Red-emitting chimeric firefly luciferase for in vivo imaging in low ATP cellular environments. *Anal. Biochem.* **2017**, *534*, 36–39.

67. Wang, W.; Zhao, Q.; Luo, M.; Li, M.; Wang, D.; Wang, Y.; Liu, Q. Immobilization of Firefly Luciferase on PVA-co-PE Nanofibers Membrane as Biosensor for Bioluminescent Detection of ATP. *ACS Appl. Mater. Interfaces* **2015**, *7*, 20046–20052.

68. Smirnova, D. V; Ugarova, N. N. Firefly Luciferase-based Fusion Proteins and their Applications in Bioanalysis. *Photochem. Photobiol.* **2017**, *93*, 436–447.

69. Adams, S. T.; Miller, S. C. Beyond D-luciferin: Expanding the Scope of Bioluminescence Imaging in vivo. *Curr. Opin. Chem. Biol.* **2014**, *0*, 112–120.

70. Simonyan, H.; Hurr, C.; Young, C. N. A synthetic luciferin improves in vivo bioluminescence imaging of gene expression in cardiovascular brain regions. *Physiol. Genomics* **2016**, *48*, 762–770.

71. Paulmurugan, R.; Gambhir, S. S. Monitoring Protein−Protein Interactions Using Split Synthetic Renilla Luciferase Protein-Fragment-Assisted Complementation. *Anal. Chem.* **2003**, *75*, 1584–1589.

72. Bhaumik, S.; Gambhir, S. S. Optical imaging of Renilla luciferase reporter gene expression in living mice. *Proc. Natl. Acad. Sci. U. S. A.* **2002**, *99*, 377–382.

73. Eremeeva, E. V; Markova, S. V; Vysotski, E. S. Highly active BRET-reporter based on yellow mutant of Renilla muelleri luciferase. *Dokl. Biochem. Biophys.* **2013**, *450*, 147–150.

74. Lorenz, W. W.; Cormier, M. J.; O'Kane, D. J.; Hua, D.; Escher, A. A.; Szalay, A. A. Expression of the Renilla reniformis luciferase gene in mammalian cells. *J. Biolumin. Chemilumin.* **1996**, *11*, 31–37.

75. Tannous, B. A.; Kim, D.-E.; Fernandez, J. L.; Weissleder, R.; Breakefield, X. O. Codon-Optimized Gaussia Luciferase cDNA for Mammalian Gene Expression in Culture and in Vivo. *Mol. Ther.* **2005**, *11*, 435–443.

76. Stepanyuk, G. A.; Xu, H.; Wu, C.-K.; Markova, S. V; Lee, J.; Vysotski, E. S.; Wang, B.-C. Expression, purification and characterization of the secreted luciferase of the copepod Metridia longa from Sf9 insect cells. *Protein Expr. Purif.* **2008**, *61*, 142–148.

77. Inoue, Y.; Sheng, F.; Kiryu, S.; Watanabe, M.; Ratanakanit, H.; Izawa, K.; Tojo, A.; Ohtomo, K. Gaussia Luciferase for Bioluminescence Tumor Monitoring in Comparison

with Firefly Luciferase. *Mol. Imaging* **2011**, *10*, 7290.2010.00057.

78. Degeling, M. H.; Bovenberg, M. S. S.; Lewandrowski, G. K.; de Gooijer, M. C.; Vleggeert-Lankamp, C. L. A.; Tannous, M.; Maguire, C. A.; Tannous, B. A. Directed molecular evolution reveals Gaussia luciferase variants with enhanced light output stability. *Anal. Chem.* **2013**, *85*, 3006–3012.

79. Thompson, E. M.; Nagata, S.; Tsuji, F. I. Cloning and expression of cDNA for the luciferase from the marine ostracod Vargula hilgendorfii. *Proc. Natl. Acad. Sci. U. S. A.* **1989**, *86*, 6567–6571.

80. Thompson, E. M.; Nagata, S.; Tsuji, F. I. Vargula hilgendorfii luciferase: a secreted reporter enzyme for monitoring gene expression in mammalian cells. *Gene* **1990**, *96*, 257–262.

81. Hunt, E. A.; Moutsiopoulou, A.; Broyles, D.; Head, T.; Dikici, E.; Daunert, S.; Deo, S. K. Expression of a soluble truncated Vargula luciferase in Escherichia coli. *Protein Expr. Purif.* **2017**, *132*, 68–74.

82. Tanahashi, Y.; Ohmiya, Y.; Honma, S.; Katsuno, Y.; Ohta, H.; Nakamura, H.; Honma, K. I. Continuous measurement of targeted promoter activity by a secreted bioluminescence reporter, Vargula hilgendorfii luciferase. *Anal. Biochem.* **2001**, *289*, 260–266.

83. Markova, S. V; Golz, S.; Frank, L. A.; Kalthof, B.; Vysotski, E. S. Cloning and Expression of cDNA for a Luciferase from the Marine Copepod Metridia longa A NOVEL SECRETED BIOLUMINESCENT REPORTER ENZYME. *J. Biol. Chem.* **2004**, *279*, 3212–3217.

84. Song, G.; Wu, Q.-P.; Xu, T.; Liu, Y.-L.; Xu, Z.-G.; Zhang, S.-F.; Guo, Z.-Y. Quick preparation of nanoluciferase-based tracers for novel bioluminescent receptor-binding assays of protein hormones: Using erythropoietin as a model. *J. Photochem. Photobiol. B Biol.* **2015**, *153*, 311–316.

85. Hall, M. P.; Unch, J.; Binkowski, B. F.; Valley, M. P.; Butler, B. L.; Wood, M. G.;

Otto, P.; Zimmerman, K.; Vidugiris, G.; Machleidt, T.; et al. Engineered Luciferase Reporter from a Deep Sea Shrimp Utilizing a Novel Imidazopyrazinone Substrate. *ACS Chem. Biol.* **2012**, *7*, 1848–1857.

86. He, S.-X.; Song, G.; Shi, J.-P.; Guo, Y.-Q.; Guo, Z.-Y. Nanoluciferase as a novel quantitative protein fusion tag: Application for overexpression and bioluminescent receptor-binding assays of human leukemia inhibitory factor. *Biochimie* **2014**, *106*, 140–148.

87. Li, J.; Guo, Z.; Sato, T.; Yuan, B.; Ma, Y.; Qian, D.; Zhong, J.; Jin, M.; Huang, P.; Che, L.; et al. Optimized application of the secreted Nano-luciferase reporter system using an affinity purification strategy. *PLoS One* **2018**, *13*, e0196617.

88. Li, J.; Guo, Z.; Sato, T.; Yuan, B.; Ma, Y.; Qian, D.; Zhong, J.; Jin, M.; Huang, P.; Che, L.; et al. Optimized application of the secreted Nano-luciferase reporter system using an affinity purification strategy. *PLoS One* **2018**, *13*, e0196617.

89. Holzinger, M.; Le Goff, A.; Cosnier, S. Nanomaterials for biosensing applications: a review. *Front. Chem.* **2014**, *2*, 63.

90. Wu, Q.; Chu, M. Self-illuminating quantum dots for highly sensitive in vivo real-time luminescent mapping of sentinel lymph nodes. *Int. J. Nanomedicine* **2012**, *7*, 3433.

91. Tsuboi, S.; Jin, T. Recombinant Protein (Luciferase-IgG Binding Domain) Conjugated Quantum Dots for BRET-Coupled Near-Infrared Imaging of Epidermal Growth Factor Receptors. *Bioconjug. Chem.* **2018**, *29*, 1466–1474.

92. Yu, X.; Wen, K.; Wang, Z.; Zhang, X.; Li, C.; Zhang, S.; Shen, J. General Bioluminescence Resonance Energy Transfer Homogeneous Immunoassay for Small Molecules Based on Quantum Dots. *Anal. Chem.* **2016**, *88*, 3512–3520.

93. El Khamlichi, C.; Reverchon-Assadi, F.; Hervouet-Coste, N.; Blot, L.; Reiter, E.; Morisset-Lopez, S. Bioluminescence Resonance Energy Transfer as a Method to Study Protein-Protein Interactions: Application to G Protein Coupled Receptor Biology. *Molecules* **2019**, *24*, 537.

94. Stryer, L.; Haugland, R. P. Energy transfer: a spectroscopic ruler. *Proc. Natl. Acad. Sci.* **1967**, *58*, 719 LP – 726.

95. Couturier, C.; Deprez, B. Setting Up a Bioluminescence Resonance Energy Transfer High throughput Screening Assay to Search for Protein/Protein Interaction Inhibitors in Mammalian Cells. *Front. Endocrinol. (Lausanne).* **2012**, *3*, 100.

96. Borroto-Escuela, D. O.; Flajolet, M.; Agnati, L. F.; Greengard, P.; Fuxe, K. Bioluminescence resonance energy transfer methods to study G protein-coupled receptor-receptor tyrosine kinase heteroreceptor complexes. *Methods Cell Biol.* **2013**, *117*, 141–164.

97. Mild, J. G.; Fernandez, L. R.; Gayet, O.; Iovanna, J.; Dusetti, N.; Edreira, M. M. Optimization of a Bioluminescence Resonance Energy Transfer-Based Assay for Screening of Trypanosoma cruzi Protein/Protein Interaction Inhibitors. *Mol. Biotechnol.* **2018**, *60*, 369–379.

98. Rumyantsev, K. A.; Turoverov, K. K.; Verkhusha, V. V Near-infrared bioluminescent proteins for two-color multimodal imaging. *Sci. Rep.* **2016**, *6*, 36588.

99. Kojima, R.; Takakura, H.; Ozawa, T.; Tada, Y.; Nagano, T.; Urano, Y. Rational Design and Development of Near-Infrared-Emitting Firefly Luciferins Available In Vivo. *Angew. Chemie Int. Ed.* **2012**, *52*, 1175–1179.

100. Song, G.; Wu, Q.-P.; Xu, T.; Liu, Y.-L.; Xu, Z.-G.; Zhang, S.-F.; Guo, Z.-Y. Quick preparation of nanoluciferase-based tracers for novel bioluminescent receptor-binding assays of protein hormones: Using erythropoietin as a model. *J. Photochem. Photobiol. B Biol.* **2015**, *153*, 311–316.

101. Hall, M. P.; Unch, J.; Binkowski, B. F.; Valley, M. P.; Butler, B. L.; Wood, M. G.; Otto, P.; Zimmerman, K.; Vidugiris, G.; Machleidt, T.; et al. Engineered Luciferase Reporter from a Deep Sea Shrimp Utilizing a Novel Imidazopyrazinone Substrate. *ACS Chem. Biol.* **2012**, *7*, 1848–1857.

102. He, S.-X.; Song, G.; Shi, J.-P.; Guo, Y.-Q.; Guo, Z.-Y. Nanoluciferase as a novel

quantitative protein fusion tag: Application for overexpression and bioluminescent receptor-binding assays of human leukemia inhibitory factor. *Biochimie* **2014**, *106*, 140–148.

103. Wu, Y.; Chakrabortty, S.; Gropeanu, R. A.; Wilhelmi, J.; Xu, Y.; Er, K. S.; Kuan, S. L.; Koynov, K.; Chan, Y.; Weil, T. pH-Responsive Quantum Dots via an Albumin Polymer Surface Coating. *J. Am. Chem. Soc.* **2010**, *132*, 5012–5014.

104. Liu, H.-B.; Yan, Q.; Wang, C.; Liu, X.; Wang, C.; Zhou, X.-H.; Xiao, S.-J. Saccharide- and temperature-responsive polymer brushes grown on gold nanoshells for controlled release of diols. *Colloids Surfaces A Physicochem. Eng. Asp.* **2011**, *386*, 131–134.

105. Song, F.; Tang, P. S.; Durst, H.; Cramb, D. T.; Chan, W. C. W. Nonblinking Plasmonic Quantum Dot Assemblies for Multiplex Biological Detection. *Angew. Chemie Int. Ed.* **2012**, *51*, 8773–8777.

106. Gill, R.; Zayats, M.; Willner, I. Semiconductor quantum dots for bioanalysis. *Angew. Chem. Int. Ed. Engl.* **2008**, *47*, 7602–7625.

107. Alivisatos, A. P.; Gu, W.; Larabell, C. Quantum dots as cellular probes. *Annu. Rev. Biomed. Eng.* **2005**, *7*, 55–76.

108. Gerion, D.; Pinaud, F.; Williams, S. C.; Parak, W. J.; Zanchet, D.; Weiss, S.; Alivisatos, A. P. Synthesis and Properties of Biocompatible Water-Soluble Silica-Coated CdSe/ZnS Semiconductor Quantum Dots. *J. Phys. Chem. B* **2001**, *105*, 8861–8871.

109. Aubert, T.; Soenen, S. J.; Wassmuth, D.; Cirillo, M.; Van Deun, R.; Braeckmans, K.; Hens, Z. Bright and Stable CdSe/CdS@SiO2 Nanoparticles Suitable for Long-Term Cell Labeling. *ACS Appl. Mater. Interfaces* **2014**, *6*, 11714–11723.

110. Aubert, T.; Grasset, F.; Mornet, S.; Duguet, E.; Cador, O.; Cordier, S.; Molard, Y.; Demange, V.; Mortier, M.; Haneda, H. Functional silica nanoparticles synthesized by water-in-oil microemulsion processes. *J. Colloid Interface Sci.* **2010**, *341*, 201–208.

111. Schaufele, F.; Demarco, I.; Day, R. N. FRET Imaging in the Wide-Field Microscope. In *Molecular Imaging*; PERIASAMY, A.; DAY, R. N. B. T.-M. I., Eds.; American Physiological Society: San Diego, 2005; pp. 72–94.

112. Selvan, S. T.; Tan, T. T.; Ying, J. Y. Robust, Non-Cytotoxic, Silica-Coated CdSe Quantum Dots with Efficient Photoluminescence. *Adv. Mater.* **2005**, *17*, 1620–1625.

113. De, A.; Loening, A. M.; Gambhir, S. S. An improved bioluminescence resonance energy transfer strategy for imaging intracellular events in single cells and living subjects. *Cancer Res.* **2007**, *67*, 7175–7183.

114. Venisnik, K. M.; Olafsen, T.; Loening, A. M.; Iyer, M.; Gambhir, S. S.; Wu, A. M. Bifunctional antibody-Renilla luciferase fusion protein for in vivo optical detection of tumors. *Protein Eng. Des. Sel.* **2006**, *19*, 453–460.

115. Dacres, H.; Michie, M.; Wang, J.; Pfleger, K. D. G.; Trowell, S. C. Effect of enhanced Renilla luciferase and fluorescent protein variants on the Forster distance of Bioluminescence resonance energy transfer (BRET). *Biochem. Biophys. Res. Commun.* **2012**, *425*, 625–629.

116. Alam, R.; Karam, L. M.; Doane, T. L.; Coopersmith, K.; Fontaine, D. M.; Branchini, B. R.; Maye, M. M. Probing Bioluminescence Resonance Energy Transfer in Quantum Rod-Luciferase Nanoconjugates. *ACS Nano* **2016**, *10*, 1969–1977.

117. Nie, S.; Emory, S. R. Probing Single Molecules and Single Nanoparticles by Surface-Enhanced Raman Scattering. *Science (80-.).* **1997**, *275*, 1102 LP – 1106.

118. Bishop, K. J. M.; Wilmer, C. E.; Soh, S.; Grzybowski, B. A. Nanoscale forces and their uses in self-assembly. *Small* **2009**, *5*, 1600–1630.

119. Dabbousi, B. O.; Rodriguez-Viejo, J.; Mikulec, F. V; Heine, J. R.; Mattoussi, H.; Ober, R.; Jensen, K. F.; Bawendi, M. G. (CdSe)ZnS Core−Shell Quantum Dots: Synthesis and Characterization of a Size Series of Highly Luminescent Nanocrystallites. *J. Phys. Chem. B* **1997**, *101*, 9463–9475.

120. Yang, R. S. H.; Chang, L. W.; Wu, J.-P.; Tsai, M.-H.; Wang, H.-J.; Kuo, Y.-C.; Yeh, T.-K.; Yang, C. S.; Lin, P. Persistent Tissue Kinetics and Redistribution of Nanoparticles, Quantum Dot 705, in Mice: ICP-MS Quantitative Assessment. *Environ. Health Perspect.* **2007**, *115*, 1339–1343.

121. Widy-Tyszkiewicz, E.; Piechal, A.; Gajkowska, B.; Śmiałek, M. Tellurium-induced cognitive deficits in rats are related to neuropathological changes in the central nervous system. *Toxicol. Lett.* **2002**, *131*, 203–214.

122. Vinceti, M.; Wei, E. T.; Malagoli, C.; Bergomi, M.; Vivoli, G. Adverse health effects of selenium in humans. *Rev. Environ. Health* 2001, *16*, 233–251.

123. UMEMURA, T. Experimental reproduction of itai-itai disease, a chronic cadmium poisoning of humans, in rats and monkeys. *Jpn. J. Vet. Res.* **2000**, *48*, 15–28.

124. Bertin, G.; Averbeck, D. Cadmium: cellular effects, modifications of biomolecules, modulation of DNA repair and genotoxic consequences (a review). *Biochimie* **2006**, *88*, 1549–1559.

125. Sukhanova, A.; Bozrova, S.; Sokolov, P.; Berestovoy, M.; Karaulov, A.; Nabiev, I. Dependence of Nanoparticle Toxicity on Their Physical and Chemical Properties. *Nanoscale Res. Lett.* **2018**, *13*, 44.

126. Hardman, R. A Toxicologic Review of Quantum Dots: Toxicity Depends on Physicochemical and Environmental Factors. *Environ. Health Perspect.* **2006**, *114*, 165–172.

127. Xu, G.; Lin, G.; Lin, S.; Wu, N.; Deng, Y.; Feng, G.; Chen, Q.; Qu, J.; Chen, D.; Chen, S.; et al. The Reproductive Toxicity of CdSe/ZnS Quantum Dots on the in vivo Ovarian Function and in vitro Fertilization. **2016**, *6*, 37677.

128. Liu, J.; Yang, C.; Liu, J.; Hu, R.; Hu, Y.; Chen, H.; Law, W.-C.; Swihart, M. T.; Ye, L.; Wang, K.; et al. Effects of Cd-based Quantum Dot Exposure on the Reproduction and Offspring of Kunming Mice over Multiple Generations. **2017**, *1*, 23–37.

129. Reyes-Esparza, J.; Martínez-Mena, A.; Gutiérrez-Sancha, I.; Rodríguez-Fragoso, P.; de la Cruz, G. G.; Mondragón, R.; Rodríguez-Fragoso, L. Synthesis, characterization and biocompatibility of cadmium sulfide nanoparticles capped with dextrin for in vivo and in vitro imaging application. **2015**, *13*, 83.

130. Bargheer, D.; Giemsa, A.; Freund, B.; Heine, M.; Waurisch, C.; Stachowski, G. M.; Hickey, S. G.; Eychmüller, A.; Heeren, J.; Nielsen, P. The distribution and degradation of radiolabeled superparamagnetic iron oxide nanoparticles and quantum dots in mice. *Beilstein J. Nanotechnol.* **2015**, *6*, 111–123.

131. Xiong, L.; Shuhendler, A. J.; Rao, J. Self-luminescing BRET-FRET near-infrared dots for in vivo lymph-node mapping and tumour imaging. *Nat. Commun.* **2012**, *3*, 1193.

132. Yao, J.; Li, P.; Li, L.; Yang, M. Biochemistry and biomedicine of quantum dots: from biodetection to bioimaging, drug discovery, diagnostics, and therapy. *Acta Biomater.* **2018**, *74*, 36–55.

133. Alam, R.; Zylstra, J.; Fontaine, D. M.; Branchini, B. R.; Maye, M. M. Novel multistep BRET-FRET energy transfer using nanoconjugates of firefly proteins, quantum dots, and red fluorescent proteins. *Nanoscale* **2013**, *5*, 5303–5306.

134. Kamkaew, A.; Sun, H.; England, C. G.; Cheng, L.; Liu, Z.; Cai, W. Quantum dot–NanoLuc bioluminescence resonance energy transfer enables tumor imaging and lymph node mapping in vivo. *Chem. Commun.* **2016**, *52*, 6997–7000.

135. Kumar, M.; Zhang, D.; Broyles, D.; Deo, S. K. A rapid, sensitive, and selective bioluminescence resonance energy transfer (BRET)-based nucleic acid sensing system. *Biosens. Bioelectron.* **2011**, *30*, 133–139.

136. Tsuboi, S.; Jin, T. Bioluminescence Resonance Energy Transfer (BRET)-coupled Annexin V-functionalized Quantum Dots for Near-Infrared Optical Detection of Apoptotic Cells. *ChemBioChem* **2017**, *18*, 2231–2235.

137. Kosaka, N.; Mitsunaga, M.; Bhattacharyya, S.; Miller, S. C.; Choyke, P. L.; Kobayashi, H. Self-illuminating in vivo lymphatic imaging using a bioluminescence

resonance energy transfer quantum dot nano-particle. *Contrast Media Mol. Imaging* **2011**, *6*, 55–59.

138. Feugang, J. M.; Youngblood, R. C.; Greene, J. M.; Fahad, A. S.; Monroe, W. A.; Willard, S. T.; Ryan, P. L. Application of quantum dot nanoparticles for potential non-invasive bio-imaging of mammalian spermatozoa. *J. Nanobiotechnology* **2012**, *10*, 45.

139. Wu, S.; Dou, J.; Zhang, J.; Zhang, S. A simple and economical one-pot method to synthesize high-quality water soluble CdTe QDs. *J. Mater. Chem.* **2012**, *22*, 14573–14578.

140. Chen, Y.; Guo, X.; Tse, W. H.; Sham, T.-K.; Zhang, J. Magnetic anisotropy induced in NiCo granular nanostructures by ZnO nanorods deposited on a polymer substrate. *RSC Adv.* **2014**, *4*, 47987–47991.

141. Sjöback, R.; Nygren, J.; Kubista, M. Absorption and fluorescence properties of fluorescein. *Spectrochim. Acta Part A Mol. Biomol. Spectrosc.* **1995**, *51*, L7–L21.

142. Cammarata, C. R.; Hughes, M. E.; Ofner 3rd, C. M. Carbodiimide induced cross-linking, ligand addition, and degradation in gelatin. *Mol. Pharm.* **2015**, *12*, 783–793.

143. Bah, A.; Lim, K. Y.; Wei, F.; Khursheed, A.; Sow, C. H. Fluorescence Invigoration in Carbon-Incorporated Zinc Oxide Nanowires from Passage of Field Emission Electrons. *Sci. Rep.* **2019**, *9*, 9671.

Appendices

1. Characterization of CdTe QDs

CdTe QDs were characterized using TEM imaging by my colleague, Dr. Yi Chen, a pos-doc fellow in our group (Figure 1). Photoluminescence of the CdTe QDs was observed using an excitation wavelength of 480nm and the peak excitation was observed at 580nm (Figure 2).

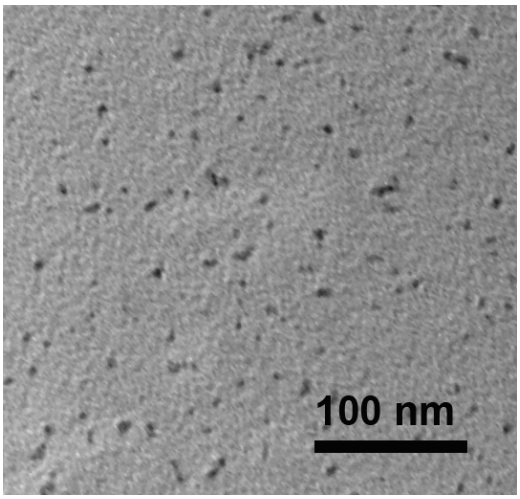

Figure 1. TEM micrograph of CdTe QDs. Average particle size is estimated to be around 10 ± 3nm.

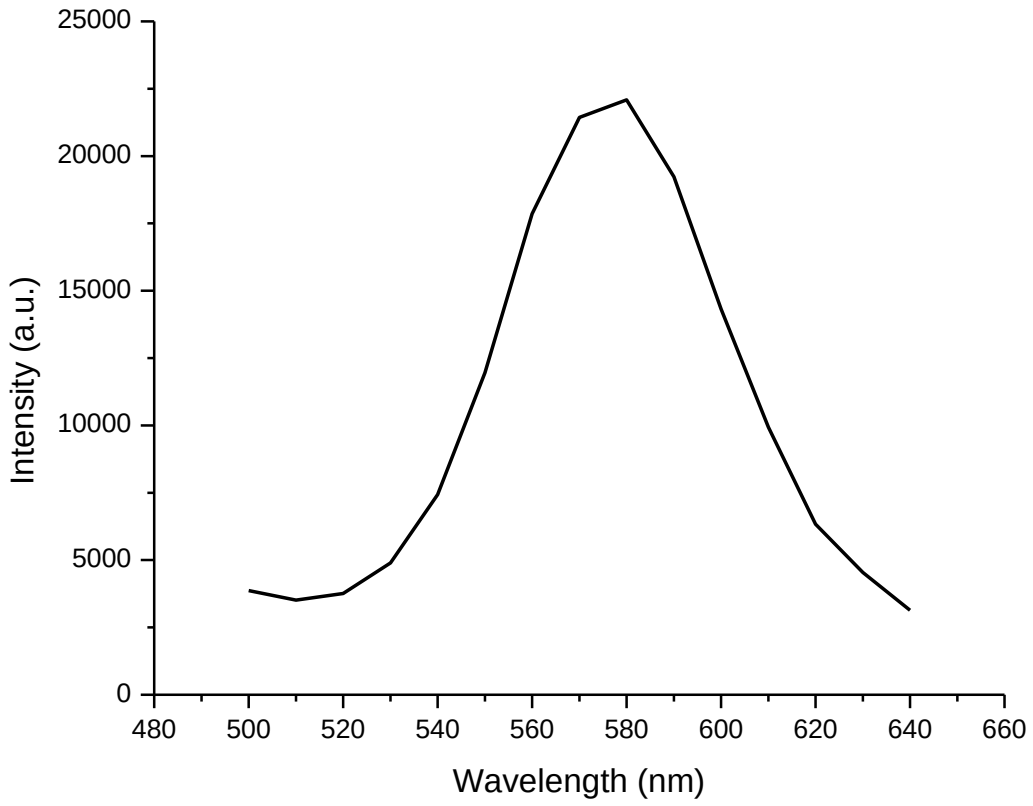

Figure 2. Photoluminescence emission spectra of CdTe QDs excited by excitation wavelength of 480nm.

2. Initial bioluminescence testing

The photoluminescence spectra of the TGA coated CdTe QDs refluxed for 2 hours show a strong emission peak at 580nm. These QDs were chosen in order to make sure the peaks of the QD and the protein do not overlap but are not too far that the signal of the protein will decay before reaching it. Increasing the reflux time shifts the emission spectra of the quantum dots to longer wavelengths due the increasing size of the CdTe QDs, which are a consequence of quantum confinement.

The photoluminescence spectra of the recombinant protein was found to have a large peak centered at 480 nm. This is expected because *Renilla* luciferase has been well documented to emit light within this region. The photoluminescence spectra of the recombinant protein bioconjugated to the CdTe QDs was found have a strong peak at 480 nm, however a

broader tail is observed in the region after 480 nm, which corresponds with the QD emission. The quantum dot emission is not strong enough to display a peak when compared to the luciferase emission, therefore this results in a broader tail.

Bioluminescence intensity was tested using two samples with identical ratios of GBP-Rluc to QD, conjugation time, and EDC concentration. The only difference being that one sample was filtered through an Amicon Ultra centrifugal filters (MWCO 100kDa, Millipore Inc.). This was to verify the solution was indeed filtered of free particles. The results indicate a significant decrease in bioluminescence upon filtering due to the filtering of free GBP-Rluc and QD particles (Appendix 1)

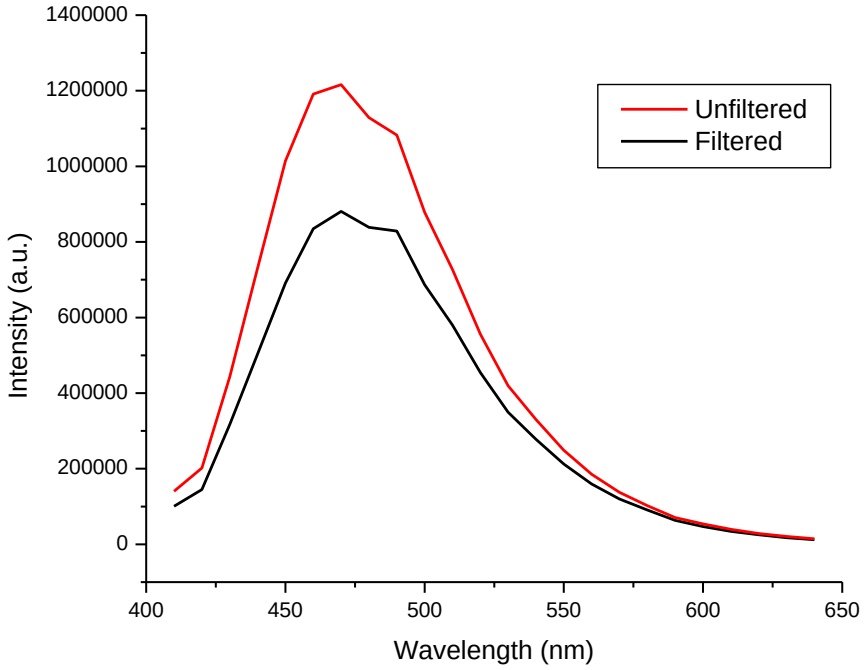

Figure 3: Bioluminescence intensity for two samples using identical conditions except for one sample is filtered and the other left unfiltered.

Curriculum Vitae

Name:	Eugene Hwang
Post-secondary Education and Degrees:	Western University London, Ontario, Canada 2012-2017 B.MSc. Western University London, Ontario, Canada 2017-2019 M.ESc.
Honours and Awards:	Western Graduate Research Scholarship 2017-2019 MITACS Accelerate Fellowship 2018-2019
Related Work Experience	Teaching Assistant The University of Western Ontario 2017-2018

Publications:

Chen Longyi, Hwang Eugene, Zhang Jin. (2018). Fluorescent Nanobiosensors for Sensing Glucose. Sensors. 18(5), 1440

Hwang Eugene, Song Ji Su, Zhang Jin. (2019). Integration of Nanomaterials and Bioluminescence Resonance Energy Transfer Techniques for Sensing Biomolecules. Biosensors, 9(1), 42